
Hydraulic and Thermal Properties of Soil Samples from the Buried Waste Test Facility

A. Cass
G. S. Campbell
T. L. Jones

October 1981

Prepared for the U.S. Department of Energy
under Contract DE-AC06-76RLO 1830

Pacific Northwest Laboratory
Operated for the U.S. Department of Energy
by Battelle Memorial Institute



NOTICE

This report was prepared as an account of work sponsored by the United States Government. Neither the United States nor the Department of Energy, nor any of their employees, nor any of their contractors, subcontractors, or their employees, makes any warranty, express or implied, or assumes any legal liability or responsibility for the accuracy, completeness or usefulness of any information, apparatus, product or process disclosed, or represents that its use would not infringe privately owned rights.

The views, opinions and conclusions contained in this report are those of the contractor and do not necessarily represent those of the United States Government or the United States Department of Energy.

PACIFIC NORTHWEST LABORATORY
operated by
BATTELLE
for the
UNITED STATES DEPARTMENT OF ENERGY
Under Contract DE-AC06-76RLO 1830

Printed in the United States of America
Available from
National Technical Information Service
United States Department of Commerce
5285 Port Royal Road
Springfield, Virginia 22151

Price: Printed Copy \$ _____*; Microfiche \$3.00

*Pages	NTIS Selling Price
001-025	\$4.00
026-050	\$4.50
051-075	\$5.25
076-100	\$6.00
101-125	\$6.50
126-150	\$7.25
151-175	\$8.00
176-200	\$9.00
201-225	\$9.25
226-250	\$9.50
251-275	\$10.75
276-300	\$11.00

HYDRAULIC AND THERMAL PROPERTIES
OF SOIL SAMPLES FROM THE BURIED
WASTE TEST FACILITY

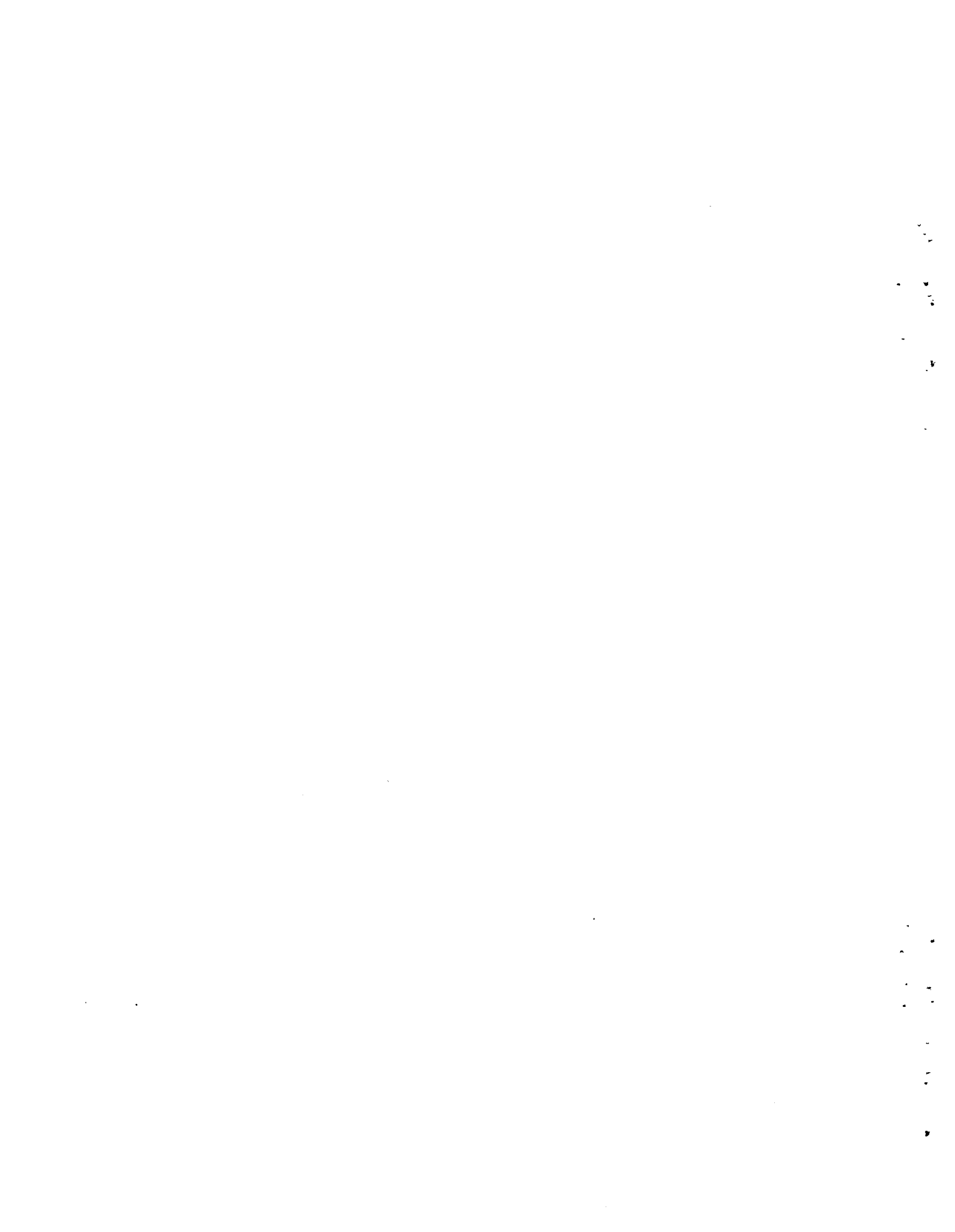
A. Cass(a)
G. S. Campbell(a)
T. L. Jones

October 1981

Prepared for
the U.S. Department of Energy
under Contract DE-AC06-76RL0 1830

Pacific Northwest Laboratory
Richland, Washington 99352

(a) Washington State University, Pullman, Washington



SUMMARY

The Department of Energy's (DOE) Low-Level Waste Management Program is providing the technology necessary to properly dispose of low-level radioactive waste. As part of this effort, Pacific Northwest Laboratory (PNL) is studying soil water movement in arid regions, as it applies to shallow land burial technology.

Shallow land burial, the most common disposal method for low-level waste, places waste containers in shallow trenches and covers them with natural sediment material. To design such a facility requires an in-depth understanding of the infiltration and evaporation processes taking place at the soil surface and the effect these processes have on the amount of water cycling through a burial zone. At the DOE Hanford Site in Richland, Washington, a field installation called the Buried Waste Test Facility (BWTF) has been constructed to study unsaturated soil water and contaminant transport. PNL is collecting data at the BWTF to help explain soil water movement at shallow depths, and specifically evaporation from bare soils. The data presented here represent the initial phase of a cooperative effort between PNL and Washington State University to use data collected at the BWTF to study the evaporation process and how it relates to the design of shallow land burial grounds.

The method of characterizing evaporation from bare soils, being evaluated in the current study with Washington State University (WSU), involves calculating, what is called, the coupled flow of mass and energy. In most flow calculations, this "coupling" is ignored; however, evaporation is one process where such a simplification may not be justified. The WSU effort is, therefore, designed to consider coupling when evaluating evaporation from bare soils. The goal of this initial phase has been to use samples of soil from the BWTF to measure transport coefficients and soil properties that are fundamental to the analysis of evaporation.

This report briefly discusses the theory of heat and water flow to illustrate the importance of the coefficients and properties measured. Materials and methods used in the laboratory analyses are described and referenced. The transport coefficients that were measured are those needed to describe the

uncoupled or independent flow of heat and water. Future work will include calculation of the additional coefficients needed to describe the coupling and interaction of heat and water flow, and the application of this analysis to describing evaporation at the BWTF. The properties and coefficients measured include soil characteristic function, hydraulic conductivity, thermal conductivity, bulk density, and particle size distribution.

The soil characteristic function shows that the BWTF soil can be drained to a saturation ratio of 0.4 at a water potential of only -3.0 J/kg. This is consistent with the particle size distribution measured. The S-shaped curve generated is difficult to describe analytically with standard equations; however, the midrange water contents can be expressed as a function of water potential using standard power functions. If the entire curve including low and high water contents are to be described, more complicated equations must be used. One approach is to allow the residual water content term of the power function to vary with potential. Analytic expressions can be obtained which allow the calculation of the soil water diffusivity.

The hydraulic conductivity may be described by the power function approach with the saturated conductivity being measured by standard procedures. The conductivity data reported here is consistent with other data reported for similar soils found on the Hanford site.

Thermal conductivity measurements are consistent with predicted trends. The increasing values with increasing data content and the range of values are indicative of sandy soils. An analytic expression is given which provides an empirical, but accurate method of describing the thermal conductivity and for calculating the thermal diffusivity.

CONTENTS

SUMMARY	iii
1.0 INTRODUCTION	1.1
2.0 THEORETICAL BACKGROUND	2.1
2.1 SOIL WATER FLOW AND TRANSPORT COEFFICIENTS	2.2
2.2 SOIL HEAT FLOW AND TRANSPORT COEFFICIENTS	2.5
2.3 SOIL PHYSICAL PROPERTIES AFFECTING HEAT AND WATER FLOW	2.7
3.0 METHODS AND MATERIALS	3.1
3.1 SOIL DESCRIPTION	3.1
3.2 SOIL DENSITY	3.2
3.3 PARTICLE SIZE DISTRIBUTION	3.2
3.4 SOIL WATER CHARACTERISTIC FUNCTION	3.2
3.4.1 Hanging Water Column	3.3
3.4.2 Pressure Plate Apparatus	3.4
3.4.3 Thermocouple Psychrometry	3.4
3.5 SATURATED HYDRAULIC CONDUCTIVITY	3.4
3.6 THERMAL DIFFUSIVITY AND CONDUCTIVITY	3.5
4.0 RESULTS AND DISCUSSION	4.1
4.1 SOIL PHYSICAL PROPERTIES	4.1
4.2 SOIL WATER CHARACTERISTIC CURVE	4.2
4.3 HYDRAULIC CONDUCTIVITY	4.6
4.4 THERMAL CONDUCTIVITY.	4.6
5.0 CONCLUSIONS	5.1
REFERENCES.	Ref.1

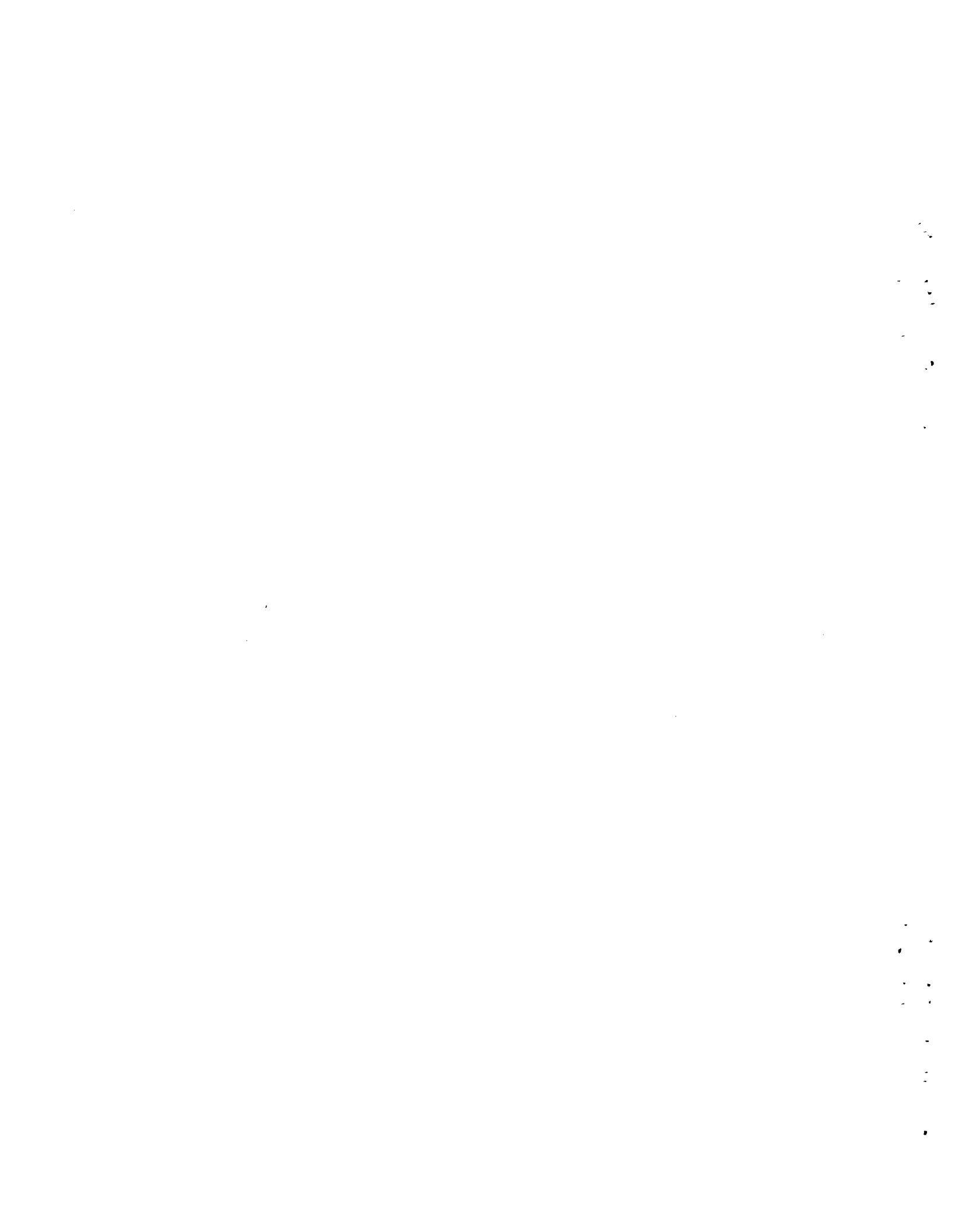
APPENDIX A: THE COUPLED FLOW OF HEAT AND WATER	A.1
A.1 FLUX OF WATER	A.1
A.2 ISOTHERMAL TRANSPORT OF WATER	A.2
A.3 THERMAL TRANSPORT OF WATER	A.5
A.4 HEAT CONDUCTION.	A.7
A.5 COUPLED HEAT AND WATER FLUX	A.7
SYMBOL NOTATION.	A.14

FIGURES

1.1	Buried Waste Test Facility	1.2
3.1	Schematic Representation of the Thermal Diffusivity Apparatus	3.7
4.1	Summation Percentage Curves for B-Soil and L-Soil	4.2
4.2	Soil Water Retention Curve for L-Soil Hanging Water Column and Pressure Plate Data	4.4
4.3	Soil Water Characteristic Curve for L-Soil	4.4
4.4	Comparison of the Soil Water Characteristic Function for B-Soil and L-Soil	4.5
4.5	Thermal Conductivity of L-Soil as a Function of Water Content, Determined Over the Temperature Range 21 to 26°C	4.7

TABLES

4.1	Physical Properties of BWTF Soil	4.1
4.2	Soil Water Retention Data for BWTF Soil Determined by Three Methods: Hanging Water Column, Pressure Plate, and Thermocouple Psychrometry	4.3
4.3	Thermal Conductivity and Diffusivity of BWTF Soil	4.7
A.1	Diagrammatic Representation and Qualitative Description of Vapor and Liquid Flow Quantities	A.8



1.0 INTRODUCTION

The Department of Energy's (DOE) Low-Level Waste Management Program is providing the technology necessary to properly dispose of low-level radioactive waste. As part of this effort, Pacific Northwest Laboratory (PNL) is studying soil water movement in arid regions, as it applies to shallow land burial technology.

Shallow land burial, the most common disposal method for low-level waste, places waste containers in shallow trenches and covers them with natural sediment material. In most arid burial grounds, the distance from the bottom of the waste zone is a significant distance from the water table, perhaps more than 100 meters. In contrast, the distance from the top of the waste zone to the ground surface may be very small--less than one meter. This upper meter of soil is generally the most active, in terms of water and heat flow, of the entire soil profile. Essentially all of the annual precipitation is cycled through this zone and sometimes water is drawn into this zone from deeper depths. Shallow land burial grounds must, therefore, be designed to minimize the amount of water allowed to drain through this upper meter into the burial zone during wet periods and also minimize the amount of water drawn up through the burial zone from deeper depths during dry periods. To design such a facility requires an in-depth understanding of the infiltration and evaporation processes taking place at the soil surface and the effect these processes have on the amount of water cycling through a burial zone. The data presented here represent the initial phase of a cooperative effort between PNL and Washington State University to better define the evaporation process and how it relates to the design of shallow land burial grounds.

At the DOE Hanford Site in Richland, Washington, a field installation called the Buried Waste Test Facility (BWTF) has been constructed to study unsaturated soil water and contaminant transport. [The facility, described in Phillips et al. (1979), is shown schematically in Figure 1.1.] PNL is collecting data at the BWTF to help explain soil water movement at shallow depths, and specifically evaporation from bare soils. The soil energy balance and thermal regime is monitored by using thermocouples throughout the facility to monitor

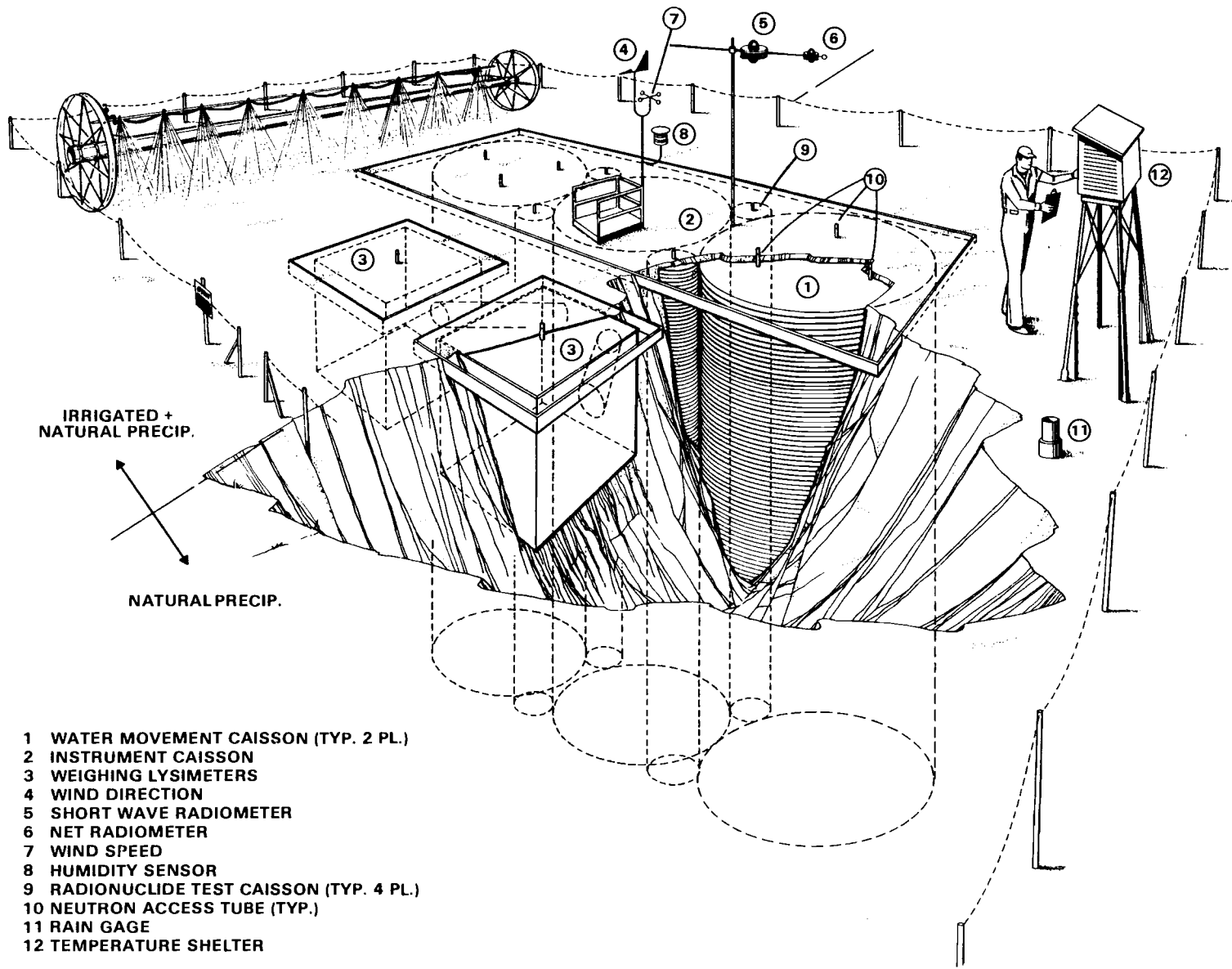
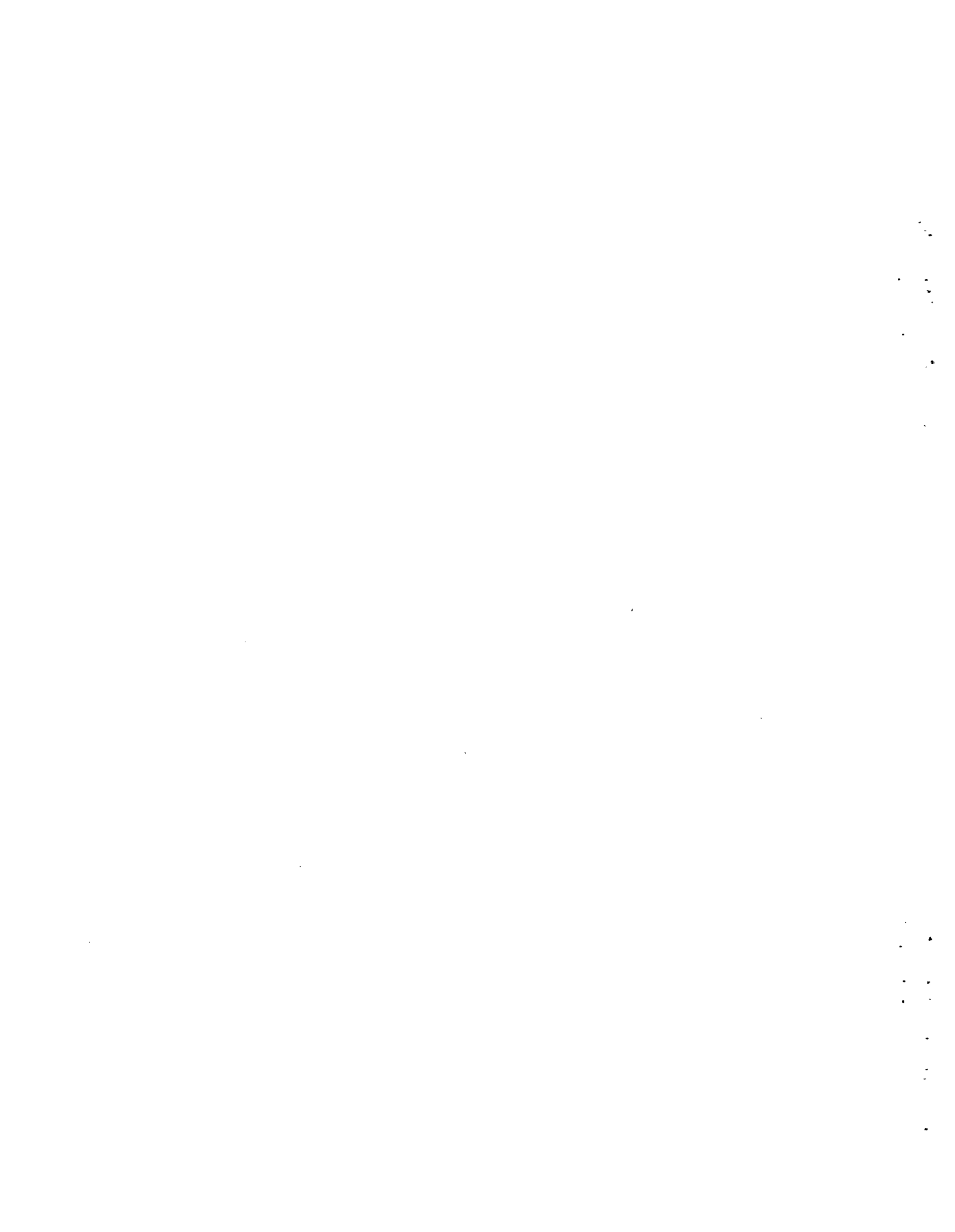


FIGURE 1.1. Buried Waste Test Facility

the response of soil temperature to incoming solar radiation, measured by both net radiometers and short-wave radiometers. The water balance is monitored with surface rain gauges to record precipitation and with neutron moisture gauges to follow changes in soil water content at depth. There are also two load-cell-type weighing lysimeters to provide direct measurements of average evaporation rates. Data recorded at the BWTF are to be used to evaluate various methods for predicting water and energy balance changes that could take place in a shallow land burial ground. Calculation procedures proven acceptable may then be used to aid the design and evaluation of burial ground cover designs.

The method of characterizing evaporation from bare soils, being evaluated in the current study with Washington State University (WSU), involves calculating, what is called, the coupled flow of mass and energy. The mass referred to is water, either as a liquid or a vapor, and the energy is in the form of both latent and sensible heat. The flow is said to be coupled because an imbalance in either heat or water content will cause both quantities to be redistributed. The mathematical implication is that equations describing soil heat flow and soil water flow must be solved simultaneously. To be completely rigorous, water flow may not be fully characterized without accounting for the concurrent flow of heat and vice-versa. In most flow calculations, this "coupling" is ignored; however, evaporation is one process where such a simplification may not be justified. The WSU effort is, therefore, designed to consider coupling when evaluating evaporation from bare soils.

This report briefly discusses the theory of heat and water flow to illustrate the importance of the coefficients and properties measured. Materials and methods used in the laboratory analyses are described and referenced. The transport coefficients that were measured are those needed to describe the uncoupled or independent flow of heat and water. Future work will include calculation of the additional coefficients needed to describe the coupling and interaction of heat and water flow, and the application of this analysis to describing evaporation at the BWTF. The properties and coefficients measured include soil characteristic function, hydraulic conductivity, thermal conductivity, bulk density, and particle size distribution.



2.0 THEORETICAL BACKGROUND

At the soil surface, water is added by infiltration and lost through evaporation. At arid sites, the infiltration is assumed equal to the precipitation (i.e., no runoff), which is an easily measured quantity. Actual evaporation is, however, very difficult to accurately measure or predict. Potential evaporation, the measured evaporation from a free water surface, is often reported as evaporation; however, actual evaporation from bare soils may only be 30% of the annual potential rate. The rate of actual evaporation is a function of the amount of energy available for the vaporization process, and the rate at which water moves up to the soil surface. This process is difficult to quantify as it involves a complicated coupling of the transport of heat and water within the upper part of the soil profile.

In many studies, heat flow and water flow through soils are treated as two independent processes. That is, heat flow is not considered when calculating soil water flow, and water flow is not considered when calculating heat flow. For most applications, the interaction or coupling between the two flow components accounts for a small percentage of the total flow and the simpler analysis is appropriate. However, in this study coupled flow analysis is used to better characterize the evaporation process.

The material presented here describes the transport coefficients and soil properties that are common to both the coupled and uncoupled analysis. The equations presented in the main text are those used for the uncoupled analysis and serve to illustrate the meaning and origin of the coefficients measured. When analyzing the coupled effect of heat and water flow, extra terms describing the interactions between heat and water must be added to the basic equations and extra coefficients included; however, the relationships between coefficients and the physical principles described here remain valid. [See Appendix A for the additional parameters needed to perform the coupled analysis of heat and water flow.] First, equations describing the flow of water as a function of water content or water potential gradients are presented, along with transport coefficients. Then the flow of heat and the corresponding

transport coefficients are described as a function of soil temperature gradients. Finally, soil physical properties that affect heat and water flow are discussed.

2.1 SOIL WATER FLOW AND TRANSPORT COEFFICIENTS

The equations used to describe the transport of water or heat may be classified as conservation equations. A conservation equation is the result of combining a constitutive equation with the law of continuity. The constitutive equation, which describes the physical law that governs the flow, is combined with the law of continuity to ensure that mass and energy will be conserved. The constitutive equation most commonly used to describe water flow is Darcy's law. The law states that the flux of water (i.e., the amount of water flowing through a unit cross-sectional area per unit time) is proportional to the pressure drop across the soil. For one dimension, this is represented as:

$$J_w = -k \frac{\Delta P}{\Delta x} \quad (2.1)$$

where J_w = flux of water

k = hydraulic conductivity

ΔP = difference in soil water pressure

Δx = distance in soil where pressure drop is measured.

Darcy's law was used originally to describe one-dimensional horizontal flow in saturated systems (i.e., all the soil air spaces are filled with water). In this case the constant of proportionality "k" is really a constant. Darcy's law has been extended to unsaturated systems by modifying both terms on the right side of the equation. First, the soil water pressure, which is negative, is referred to as soil water potential (ψ); and second, the hydraulic conductivity is no longer a constant but a function of the water potential. The extended form of Darcy's law for one dimension then becomes:

$$J_w = -k(\psi) \frac{\partial \psi}{\partial x} \quad (2.2)$$

Equation 2.2 then serves as a definition of the hydraulic conductivity, where the conductivity is the constant of proportionality that makes equation 2.2 valid for any measured flux (J_w) and water potential gradient ($\partial\psi/\partial x$).

The law of continuity can be simply stated as:

$$\begin{array}{rcl} \text{change in storage} & & \text{flux of that} \\ \text{of some component} & = & \text{component} \\ \text{(i.e., mass, energy} & & \text{into the unit} \\ \text{etc.) per unit} & & \text{volume} \\ \text{volume} & & \text{flux of that} \\ & & \text{component} \\ & & \text{out of the} \\ & & \text{unit volume} \end{array}$$

For one-dimensional soil water flow, the differential equation becomes:

$$\frac{\partial \theta}{\partial t} = \frac{-\partial J_w}{\partial x} \quad (2.3)$$

where θ = soil water content

t = time.

Substituting equation 2.2 for J_w , the resulting conservation equation for one-dimensional horizontal soil water flow is:

$$\frac{\partial \theta}{\partial t} = \frac{\partial}{\partial x} \left(k(\psi) \frac{\partial \psi}{\partial x} \right) \quad (2.4)$$

This equation contains two independent variables, the water content (θ) and water potential (ψ). The equation may be transformed either into a water-content or water-potential-based equation by defining the soil water characteristic curve, which describes the water content as a function of water potential. Assuming that the water content/potential relationship is known, two equations can be written using the chain rule for differentiation: an equation based on water potential (equation 2.5) and an equation based on water content (equation 2.6).

$$C \frac{\partial \psi}{\partial t} = \frac{\partial}{\partial x} \left(k(\psi) \frac{\partial \psi}{\partial x} \right) \quad (2.5)$$

$$\frac{\partial \theta}{\partial t} = \frac{\partial}{\partial x} \left(\frac{1}{C} k(\theta) \frac{\partial \theta}{\partial x} \right) \quad (2.6)$$

where C = differential water capacity = $\frac{\partial \theta}{\partial \psi}$

When equation 2.6 is used, the water capacity and the hydraulic conductivity are often combined into a single transport coefficient known as the soil water diffusivity. The soil water diffusivity $D(\theta)$ is defined by:

$$D(\theta) = \frac{1}{C} k(\psi) \quad (2.7)$$

The concept of water potential, and water capacity was proposed by Buckingham (1907), while the conservation equations 2.4 and 2.5 were presented by Richards (1931). (Equation 2.5 is often referred to as the Richards equation.)

The equations shown here may be divided into two components: gradient terms or driving forces and transport coefficients. The gradient terms, such as the water content gradient ($\partial \theta / \partial x$) and the water potential gradient ($\partial \psi / \partial x$), are the forces causing flow to take place. The transport coefficients, such as water capacity (C), soil water diffusivity (D), and hydraulic conductivity (k), relate the driving force to the resulting flow rate or flux.

Equations 2.1 through 2.4 describe one-dimensional, horizontal flow. They may be extended to three dimensions and to include the effects of gravity for vertical flow; however, the relationships of the hydraulic conductivity, moisture diffusivity and water capacity would remain the same. The equations presented are sufficient to illustrate the origin and importance of transport parameters that are necessary for the uncoupled analysis.

Equations 2.1 through 2.4 are referred to as uncoupled because of the assumption that Darcy's law adequately describes the physics of soil water transport. If factors other than potential gradients should be accounted for as driving forces, such as temperature gradients, then extra terms must be incorporated into the constitutive equation (see Appendix A). When additional gradient terms are added, extra transport coefficients must be added that are appropriate to the new driving forces. The coefficients linking the flow of water to a temperature gradient and the flow of heat to a water potential gradient are referred to as the linked or coupled transport coefficients. (See Appendix A for a description of these coefficients.)

2.2 SOIL HEAT FLOW AND TRANSPORT COEFFICIENTS

The equation describing the flow of heat in soil may be derived in a way similar to that used for water flow equations. A constitutive equation, which includes the appropriate physical principles, is combined with the law of continuity. The result is a transport equation that represents heat flow as a function of all the driving forces that were chosen and also incorporates the principle of conservation of energy.

Heat is transferred in soils predominantly by conduction and convection, with water providing most of the convective transfer. The incorporation of convection into the equations provides strong coupling between the flow of heat and water. (Appendix A discusses this in detail.) For most applications the convective component can be ignored explicitly, and conduction considered alone. Therefore, this discussion is limited to conductive heat flow and identifies a list of transport coefficients analogous to those identified above for water transport. (For a discussion of the coupled or linked transport parameters, see Appendix A.)

The constitutive equation for the conduction of heat is Fourier's law of heat transfer. It states that the flux of heat (J_h) is proportional to the temperature gradient ($\partial T/\partial x$); that is,

$$J_h = -k_T \frac{\partial T}{\partial x} \quad (2.8)$$

where k_T = thermal conductivity

The similarity of equation 2.8 to Darcy's law (equation 2.1) is quite apparent. The proportionality constant k_T relates heat flux to the temperature gradient in the same way that the hydraulic conductivity relates the flow of water to the water potential gradient. The subscript "T" is used to differentiate the thermal conductivity (k_T) from the hydraulic conductivity (k).

The law of continuity applied to heat flow states that:

$$\begin{array}{l} \text{the change in heat} \\ \text{per unit volume} \end{array} = \begin{array}{l} \text{flow of heat} \\ \text{into the unit} \\ \text{volume} \end{array} - \begin{array}{l} \text{flow of heat} \\ \text{out of the} \\ \text{unit volume} \end{array}$$

In equation form, it looks very similar to equation 2.3:

$$\frac{\partial H}{\partial t} = \frac{-\partial J_h}{\partial x} \quad (2.9)$$

where H = heat or energy per unit volume

Substituting equation 2.8 for J_h , the conservation equation describing the flow of heat by conduction is

$$\frac{\partial H}{\partial t} = \frac{\partial}{\partial x} \left(k_T \frac{\partial T}{\partial x} \right) \quad (2.10)$$

This equation contains two independent variables, heat and temperature, as does equation 2.4. The most common method for reconciling these two variables is to use the concept of heat capacity (C_v). Heat capacity is defined by the following expression:

$$\frac{\partial H}{\partial t} = C_v \frac{\partial T}{\partial t} \quad (2.11)$$

where C_v = volumetric heat capacity = $\frac{\partial H}{\partial T}$

Substituting equation 2.1 into equation 2.10 gives:

$$C_v \frac{\partial T}{\partial t} = \frac{\partial}{\partial x} \left(k_T \frac{\partial T}{\partial x} \right) \quad (2.12)$$

The quantity C_v is analogous to the differential water capacity (C) in equation 2.5. The analogy between heat and water transport is carried one step further by dividing equation 2.12 by C_v and obtaining

$$\frac{\partial T}{\partial t} = \frac{\partial}{\partial x} \left(\frac{1}{C_v} k_T \frac{\partial T}{\partial x} \right) \quad (2.13)$$

The quantity $1/C_v k_T$ may be defined as the thermal diffusivity (D_{hT}) of the soil. The subscript "hT" serves to separate this parameter from the soil moisture diffusivity (D) of equation 2.7.

Soil is a composite material often containing three phases. The solid phase or matrix is generally composed of silicate minerals, often assumed to have the same thermal properties as quartz. The gas phase, present under unsaturated conditions, is a combination of air and water vapor and the third phase is the soil water. The conductivity and capacity parameters of equations 2.12 and 2.13 represent average values of the composite material. These parameters are sometimes calculated as a weighted average of the conductivities and capacities of the individual components; other times they are measured with experiments performed on bulk samples of the soil. Because the soil is a composite material, the conductivity and capacity will change as the mass ratio of the components changes. These changes are expressed as a water content dependence of the heat capacity and the thermal conductivity. There is also a temperature dependence but it is often assumed insignificant relative to the water content dependence.

The water content dependence of the soil thermal conductivity results from a complicated process involving latent heat transfer between vapor and liquid water and thermal conduction. When analyzing heat flow independently of water flow these microscopic processes are only accounted for empirically in the macroscopic thermal conductivity measurement. Examining this relationship in detail, however, provides the key to characterizing the linked transport coefficients mentioned above. Measurements of thermal conductivities at different temperatures, pressures, and water contents provide the data necessary to estimate these additional parameters.

2.3 SOIL PHYSICAL PROPERTIES AFFECTING HEAT AND WATER FLOW

A set of soil properties that determine the values of the transport coefficients are included in any analysis of heat and water transport. They do not appear explicitly in the transport equations and are therefore differentiated from transport coefficients. One such property is the soil characteristic function. This is the functional relationship between soil water potential and soil water content, and is considered the property most influential on the water flow characteristics. Soils with similar characteristic functions will also have similar hydraulic conductivity functions and a similar water content dependence of thermal conductivity. The differential water capacity,

defined by equation 2.4, is the derivative of the soil characteristic function, and methods exist for calculating the hydraulic conductivity function directly from the soil water characteristic function. The relationship between soil water content and soil water potential can often be expressed analytically. The most common expression used is the power function, where the water potential is expressed as the water content raised to some power (Brooks and Corey 1964; Campbell 1974). Several forms of this power function are in the literature and include:

$$\psi = \psi_e \left(\frac{\theta}{\theta_s} \right)^{-b} \quad 2.14$$

$$\psi = \psi_e \left(\frac{\theta - \theta_d}{\theta_s - \theta_d} \right)^{-b} \quad 2.15$$

where ψ_e = air entry potential
 θ_d = residual water content
 θ_s = saturated water content.

The air entry potential ψ_e , also known as the soil bubbling pressure, is the water potential where the soil first starts to desorb. The term $\frac{\theta}{\theta_s}$ is referred to as the relative saturation and the term $\frac{\theta - \theta_d}{\theta_s - \theta_d}$ as referred to as the reduced water content or effective saturation. The air entry potential and the saturated water content may be measured in the laboratory or the field. In some analyses the measured values are used but often these coefficients become curve fitting parameters adjusted arbitrarily to make equations 2.14 and 2.15 fit experimental data. The parameter θ_d is nearly always used in this manner.

Soil texture is another property that is important in determining the hydraulic and thermal characteristics of soil. Texture is the term used to describe the size distribution of the soil grains. Textural classes range from clay, for predominantly microscopic particles (<2 μm dia.), to silt (>2 μm and $\leq 50 \mu\text{m}$ dia.) to sand (>50 μm and <2 mm dia.), to gravel and boulders (>2 mm dia.). The soil texture is determined by measuring the percentage of sand,

silt, and clay in a sample. Soil texture, theoretically, should determine to a great extent all other physical properties. Approximate methods are available for calculating soil characteristic curves, transport coefficients and bulk density from a textural analysis. At the present time they serve only as a relative guide and a qualitative tool.

Finally soil density is the ratio of mass of soil to the volume of the soil. The density of the individual soil grains is known as the soil particle density, and the bulk density is the measure of the overall density of the soil-void composite. The higher the bulk density the less void space. The bulk density is always less than the particle density. The relationship between void space and soil density is:

$$PSR = 1 - \frac{\rho_b}{\rho_p} \quad (2.16)$$

where PSR = pore space ratio

ρ_b = bulk density

ρ_p = particle density

All transport coefficients and the soil water characteristic functions are functions of soil bulk density. The dependence is not often quantified accurately because it is a subtle effect. Bulk densities are also difficult to measure in the field, particularly at depth, and the approximate nature of field hydraulic tests are too gross to see the density effects. Laboratory columns can be packed to known densities, if extreme care is taken, and this provides the only means for examining any density dependence of transport coefficients. The bulk density is used to calculate the saturated moisture content using equation 2.16 and to convert mass-based units to volume-based units. As an example, the water content on a mass basis θ_m (kg of water/kg of soil) is converted to water content on a volume basis θ_v (kg of water/cubic meter of soil) by multiplying by the soil bulk density:

$$\theta_v = \rho_b \theta_m \quad (2.17)$$

Also the volumetric heat capacity (C_v) is related similarly to the specific heat (C_s) by the bulk density

$$C_v = \rho_b C_s \quad (2.18)$$

The measurement of these transport coefficients and soil properties is always a difficult task. Soil samples rarely give identical results when measurements are made, and samples taken from different areas across a field always show significant spatial variability. The data presented here represent best estimates of average values and should be interpreted with this in mind.

3.0 METHODS AND MATERIALS

3.1 SOIL DESCRIPTION

The soil material used to fill the BWF lysimeters is a composite of the soil and sediment excavated during construction to a depth of approximately 8.5 meters. After construction of the lysimeter array the site was backfilled with the composite material from the excavation. The lysimeters themselves were then filled with the excavated material after it was passed through a 1/2 inch screen to remove larger gravel and stones (Phillips et al. 1979).

The original 8-meter soil profile contains two distinct zones. The top 1 to 2 meters consists of eolian (wind blown) deposits while the deeper sediments are a result of the catastrophic flooding of the Pasco Basin. The surface eolian deposits were originally placed in the Winchester series by a 1919 soil survey (Kocher and Strathorn 1919). A 1966 survey (Hajek 1966) placed this soil in the Rupert series, but this has since been changed. A new soil survey is needed to establish the correct description; however, the two most probable candidates are the Quincy series, a medium sand, and the Winchester series, a coarse sand. The particle size description given by Gee and Campbell (1980) indicates that Quincy is the correct soil series. The Quincy soil has been classified as a mixed mesic xeric torripsamment. This soil has been used in other hydrologic research and has been identified as either Rupert Sand or B-soil, (Jones et al. 1979, Gee and Campbell 1980, and Gee et al. 1981).

The flood deposits found beneath the surface eolian deposits contain up to 20% gravel with the remainder being very coarse to medium sands. These glacio-fluvial sediments are commonly referred to as the Pasco Gravels (Tailman et al. 1979, Phillips et al. 1980, and Gee and Simmons 1980). These sediments are found throughout the Hanford Site and are referred to as R(B) soil by Jones et al. (1979, 1981). The medium to coarse sands referred to by Sisson and Gibbs (1979) are also from this sediment type.

The screened backfill material used in the lysimeters resembles the Quincy soil because the gravel was removed, however, it tends to contain more coarse sand. The composite material was used by Jones et al. (1979) and was identified as L-Soil. Soil samples used for the laboratory analysis in this report

were from this composite mix and represent further characterization of the L-Soil. For this characterization effort four samples were collected from the backfill material surrounding the BWTF lysimeters. These samples were mixed, passed through a 2-mm sieve, and used for all determinations except bulk density. Bulk density samples consisted of five minimally disturbed soil cores taken from the lysimeters themselves.

3.2 SOIL DENSITY

Five minimally disturbed cylindrical cores were taken from the surface of the lysimeters. The sample cores were 75.44 ± 0.103 mm in diameter and 134.04 ± 0.419 mm height, resulting in a soil volume of $5.99 \times 10^5 \text{ mm}^3 \pm 3.6 \times 10^3 \text{ mm}^3$. The material was oven dried and the soil volume was corrected for gravel. Bulk density was calculated from the equation:

$$\rho_b = \frac{\text{oven dry mass}}{\text{volume of soil cores}} \quad (3.1)$$

Particle density was measured following the method of Blake (1965).

3.3 PARTICLE SIZE DISTRIBUTION

Particle size distribution (Day 1965) was determined on subsamples of the sieved bulk sample and corrected for water content by drying in an oven at 105°C . Results of the particle size measurement were computed using the method of Gee and Bauder (1979).

3.4 SOIL WATER CHARACTERISTIC FUNCTION

Three methods were used to measure the soil water content-water potential relationship. The hanging water column method was used for potentials in the range of -1 to -20 J/kg. This method was used because of its high accuracy in this range. Pressure plate techniques were used for the intermediate ranges of -5 to -1500 J/kg. The hanging water column is not capable of reaching these dry ranges and the pressure plate is a common technique to substitute. The dry

potentials in the range of -5000 to -10,000 J/kg were made using thermocouple psychrometers. The pressure plate apparatus is of questionable value in these ranges because sample hydraulic conductivities become so low that equilibrium is not reached; however, the psychrometer technique is fast and accurate in these dry ranges.

3.4.1 Hanging Water Column

The method of Vomocil (1965) was used after placement of BWTF soil in a glass funnel on a medium rate porous plate. Soil was compacted by gentle tapping of the funnel to a bulk density of 1.6 Mg m^{-3} . Because of the possibility that the very coarse-grained BWTF soil could develop a significant contact resistance across the porous plate, a thin (5 mm) layer of fine grained soil (Salkum silty clay loam) was first placed on the plate as a slurry (water content equal to 0.75 kg/kg) followed by the BWTF soil. The hanging water columns were connected to the glass funnels through flexible tubing to form a sealed system. Water retention was measured by weighing the glass funnels over a range of water potentials from -1 to -20 J kg^{-1} . Successive mass values of the composite BWTF soil-silty clay loam column had to be corrected for the water content of the silty clay loam layer. This was achieved from an independent determination of the soil characteristic curve of Salkum soil (equation 3.2) and knowledge of the bulk density of the layer on the porous plate (1.2 Mg m^{-3}).

$$(\theta_m = 0.4937 \psi^{-0.086}) \quad (3.2)$$

where:

θ_m = water content (kg/kg)

ψ = soil water potential

This equation is in the form of equation 2.14 where

$\theta_s = 0.50$ (kg/kg)

$\psi_e = 0.94$ (J/kg)

$1/b = -0.086$

3.4.2 Pressure Plate Apparatus

Standard pressure plate apparatus was used to determine soil water retention over the potential range -5 to $1,500 \text{ J kg}^{-1}$. Discs (3.2 mm ID x 10 mm high) were formed by sectioning a tube of plexiglass into 10-mm sections, reassembling it with masking tape, and packing it with BWTF soil to a bulk density 1.60 Mg m^{-3} . The tube was disassembled into the 10 mm soil discs contained in the plexiglass rings. Because of the problem of contact resistance at the soil plate interface, a slurry of Salkum soil (2 mm layer) also preceded placement of the soil discs on the porous plate.

3.4.3 Thermocouple Psychrometry

The method of Campbell and Wilson (1972) was used to measure soil water potential over the range $-5,000$ to $-10,000 \text{ J kg}^{-1}$ using LiCl as a standard. For the water potential range -450 to $4,000 \text{ J kg}^{-1}$, using KCl as a standard. Unconsolidated soil in beakers was dried in a microwave oven and sampled periodically for water potential and gravimetric water content determinations. A bulk density of 1.6 Mg m^{-3} was assumed for these samples.

3.5 SATURATED HYDRAULIC CONDUCTIVITY

The hydraulic conductivity was modeled with a power function similar to that used for the soil characteristic function. The form chosen follows from Brooks and Corey (1964), Campbell (1974), and Bresler et al. (1978). A comparative analysis of the three methods is given in Jones et al. (1979). This type of function was shown to be effective for the sandy soils of the Hanford Site (Jones 1979, Gee et al. 1981). The power function used is:

$$k(\theta) = k_s \left(\frac{\theta - \theta_d}{\theta_s - \theta_d} \right)^\beta \quad (3.3)$$

where

k_s = saturated hydraulic conductivity

β = parameter either measured or calculated

The parameter β can be calculated from the b-value of the soil characteristic function as $\beta = 2b + 3$, [Brooks and Corey (1964) and Campbell (1974)] or set at the constant 7.2 [Bresler et al. (1978)].

When the power function approach is used, the only parameter to be measured is the saturated hydraulic conductivity. Two methods were used on the BWTF soil samples. First the falling head method of Klute (1965) was used with brass permeameters of 15-mm dia. by 200-mm high. The soil was packed into the permeameters to a bulk density of approximately 1.6 Mg M^{-3} . The following method was suggested by Bresler et al. (1978). The bottom end of a vertical soil column is placed in water and the vertical advance of the wetting front is observed. The position of the front is then graphed as a function of $t^{1/2}$. The slope (m) is then used to calculate the saturated conductivity (k_s) by:

$$k_s = 0.27 m^4 \quad (3.4)$$

The value of k_s is then substituted into equation 3.4 to calculate the unsaturated hydraulic conductivity. If hydraulic conductivity as a function of water potential is needed then the equation for the soil water characteristic function, such as equation 2.14 or 2.15 is used to make the change of variable. Dividing $k(\theta)$ by the water capacity will give the functional relationship of the soil water diffusivity from equation 2.7.

3.6 THERMAL DIFFUSIVITY AND CONDUCTIVITY

The method of Parikh et al. (1979) as modified by McInnes (1981) was used to measure the thermal diffusivity of BWTF soil using water baths at temperatures of 21.61 ± 0.01 and $26.39 \pm 0.01^\circ\text{C}$. Soil samples with a range of water contents were prepared by adding small amounts of water to soil, thoroughly mixing the soil and sieving through a 2-mm sieve. The cycle was repeated until the required amount of water had been added. Soils were stored in plastic bags sealed in large metal containers and were again thoroughly mixed prior to packing into aluminum tubes. During packing, subsamples were taken for water content determination. Soil columns were packed using a mechanical vibrating table while adding soil slowly through a funnel with a long stem. Packing

uniformity was reasonable (maximum standard deviation was 0.08 Mg m^{-3}) and the mean bulk density of different soil columns was $1.60 \pm 0.03 \text{ Mg m}^{-3}$. A thermocouple was connected to a datalogger (model CR5, Campbell Scientific Inc., Logan Utah), as illustrated in Figure 3.1. to measure the temperature difference between waterbath and the interior of the soil column. The computational method is provided by Riha et al. (1980) and McInnes (1981).

Thermal conductivity was computed from thermal diffusivity using

$$k_T = D_{hT} C_V \quad (3.5)$$

where C_V is the volumetric heat capacity of soil, computed from

$$C_V = \rho_b C_S (1-\phi) + \rho_w C_w \phi. \quad (3.6)$$

where

ρ_s = mass bulk density of the soil columns (Mg m^{-3})

C_s = specific heat of soil, assumed to be quartz,
 $2.53 \times 10^6 \text{ J Mg}^{-1}\text{K}^{-1}$ (De Vries 1963)

ϕ = total porosity ($\text{m}^3 \text{m}^{-3}$)

ρ_w = density of water (0.998 Mg m^{-3})

C_w = specific heat of water ($4.18 \times 10^6 \text{ J Mg}^{-1}\text{K}^{-1}$)

ρ_b = bulk density of soil (Mg m^{-3})

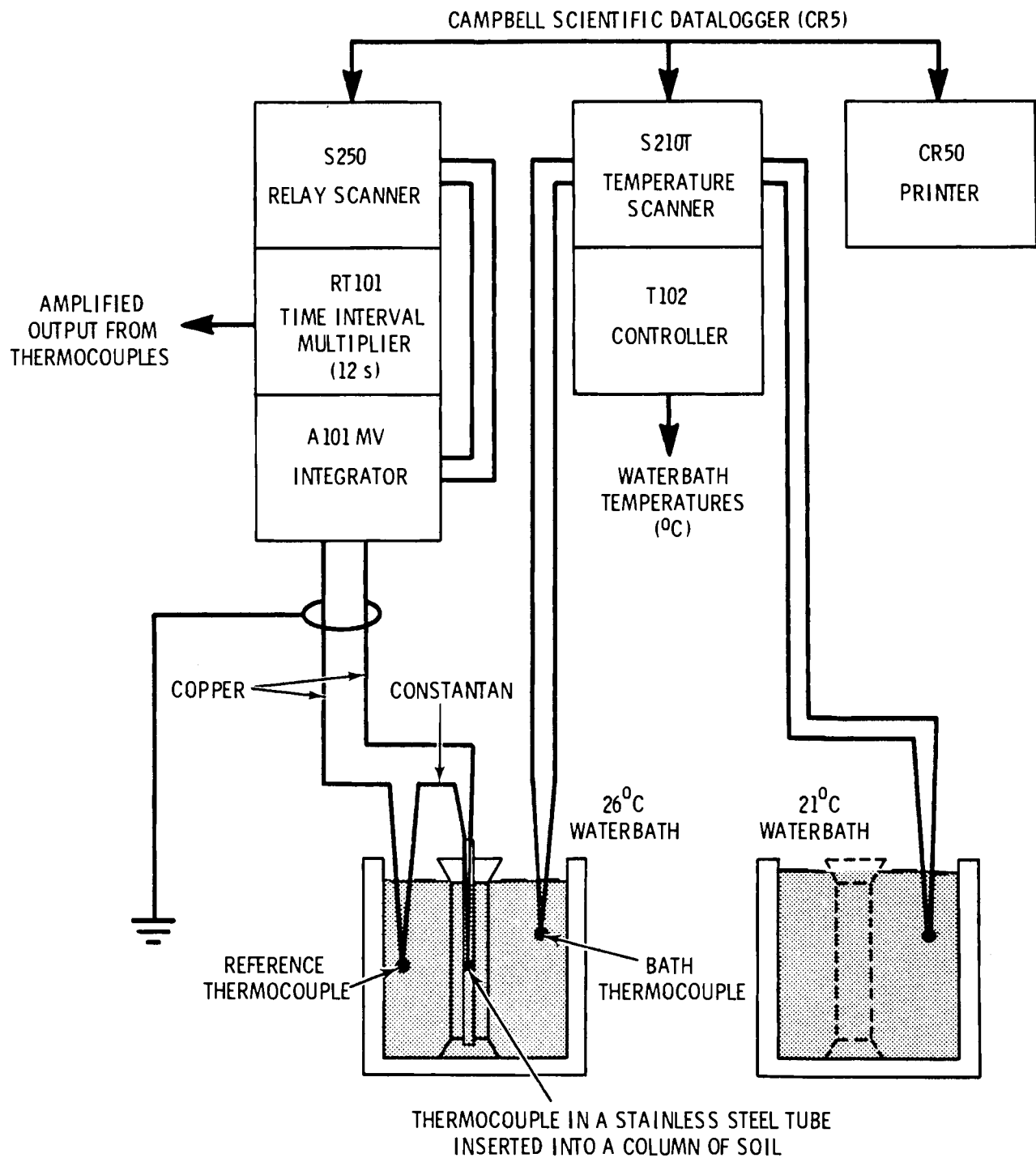


FIGURE 3.1. Schematic Representation of Thermal Diffusivity Apparatus

4.0 RESULTS AND DISCUSSION

4.1 SOIL PHYSICAL PROPERTIES

Field dry bulk density, particle density and particle size distribution shown in Table 4.1 reflect the coarse-grained, high density material comprising BWTF soil. Although all data presented here are for repacked samples with bulk density values close to 1.6 Mg m^{-3} , very little compactive effort is required to reach 1.8 Mg m^{-3} . (The hydraulic conductivity data available from Jones et al. (1979) for similar soils was obtained at bulk density values close to 1.8 Mg m^{-3} .)

Figure 4.1 shows a comparison of the particle size distribution for B-Soil (Quincy sand) and L-Soil (BWTF soil). It is apparent from the curves in Figure 4.1 and the gravel content shown in Table 4.1 that the L-soil composite mix

TABLE 4.1. Physical Properties of BWTF Soil (0 to 450 mm Depth Interval)

<u>Property</u>	<u>Fraction μm</u>	<u>Mean Value</u>	<u>Standard Deviation of the Mean</u>	<u>Unit</u>
Bulk Density	< 2000	1.54	0.0356	Mg m^{-3}
Particle Density	< 2000	2.82	0.0117	Mg m^{-3}
Gravel Content	> 2000	13.5	10.5	Mass percent of whole soil
Particle Size				
Distribution				
Clay	<2	2.3	0.05	
Silt	53 - 2	6.8	0.26	
Very fine sand	106 - 53	5.8	0.07	Mass percent of fraction less than 2 mm diameter
Fine sand	246 - 106	9.9	0.39	
Medium sand	495 - 266	32.4	0.18	
Coarse sand	1000 - 495	33.9	0.55	
Very coarse sand	2000 - 1000	7.0	0.29	
Sand content				
Very fine sand	105 - 53	6.5	-	Mass percent of sand content
Fine sand	246 - 106	11.1	-	
Medium sand	495 - 246	36.4	-	
Coarse sand	1000 - 495	38.1	-	
Very coarse sand	2000 - 1000	7.9	-	

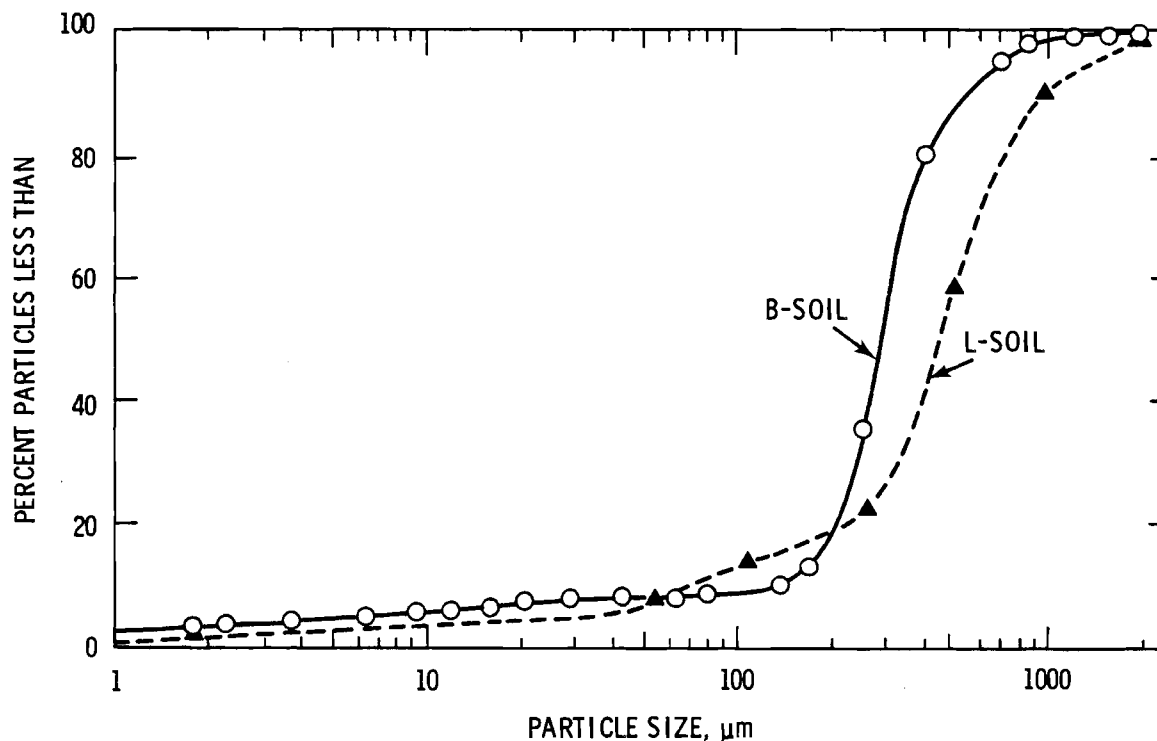


FIGURE 4.1. Summation Percentage Curves for B-Soil and L-Soil. Data for B-soil from Gee and Campbell 1980.

is coarser textured than the B-soil (Quincy). Although the soils are both classified as sands, the water flow characteristics should be somewhat different.

4.2 SOIL WATER CHARACTERISTIC CURVE

Soil water retention data are listed in Table 4.2 and plotted in Figure 4.2, 4.3, and 4.4. Figure 4.2 shows only the hanging water column and pressure plate data. The curve was drawn using Equation 2.15 with $\psi_e = 0.706 \text{ J/kg}$; $\theta_s = 0.253 \text{ kg/kg}$, $\theta_d = 0.03 \text{ kg/kg}$, and $b = 1.3$. Gee et al. (1981) used -0.1 to 10 Jkg^{-1} potential range for B-soil and estimated b to be 1.8 and 2.3 for both densities of 1.6 and 1.8, respectively. The coarser texture of the L-soil should imply a smaller b -value and so the value of 1.3 is quite reasonable for the range of potentials shown in Figure 4.2. If the entire range of potentials given in Table 4.2 is to be fit by an equation similar to 2.15, then the residual moisture content (θ_d), must be allowed to

TABLE 4.2. Soil Water Retention Data for BWTF Soil Determined by Three Methods: Hanging Water Column, Pressure Plate, and Thermocouple Psychrometry

Mass Water Content θ_m		Volume Water Content θ_v		$\frac{\theta_v}{\theta_s}$	Water Potential	Method
Mean	Standard Deviation	Mean	Standard Deviation			
kg kg ⁻¹	kg kg ⁻¹	m ³ m ⁻³	m ³ m ⁻³	-	J kg ⁻¹	
0.1006	0.0028	0.1644	0.0045	0.39	2.95	Hanging Water Column
0.0761	0.0019	0.1244	0.0030	0.30	4.93	
0.0573	0.0014	0.0937	0.0023	0.22	9.83	
0.0456	0.0005	0.0746	0.0010	0.18	13.1	
0.0397	0.0015	0.0649	0.0025	0.15	19.7	
0.0860	0.0081	0.1376	0.0129	0.32	5	Pressure Plate
0.0538	0.0041	0.0861	0.0065	0.20	10	
0.0454	0.0039	0.0727	0.0063	0.17	30	
0.0403	0.0006	0.0653	0.0019	0.15	50	
0.0367	0.0007	0.0587	0.0012	0.14	100	
0.0323	0.0011	0.0516	0.0017	0.12	483	
0.0330	0.0028	0.0528	0.0045	0.115	1000	
0.0286	0.0004	0.0457	0.0007	0.110	1500	
0.0314	-	0.0502	-	0.12	616	Thermocouple Psychrometer
0.0303	-	0.0484	-	0.11	928	
0.0254	-	0.0406	-	0.093	1168	
0.0168	-	0.0268	-	0.062	2225	
0.0224	-	0.0359	-	0.083	6410	
0.0180	-	0.0288	-	0.067	10130	
0.0139	-	0.0223	-	0.052	14620	
0.0080	-	0.0128	-	0.030	67510	

be a function of the water potential rather than a constant. Figure 4.3 shows the data in Figure 4.2 as well as the psychrometer data. The equation for the curve (solid line in Figure 4.3) is written as

$$\theta \text{ (kg/kg}^{-1}\text{)} = \frac{8}{200 + |\psi|^{0.6}} + \frac{0.3}{|\psi|^{1.3}} \quad (4.1)$$

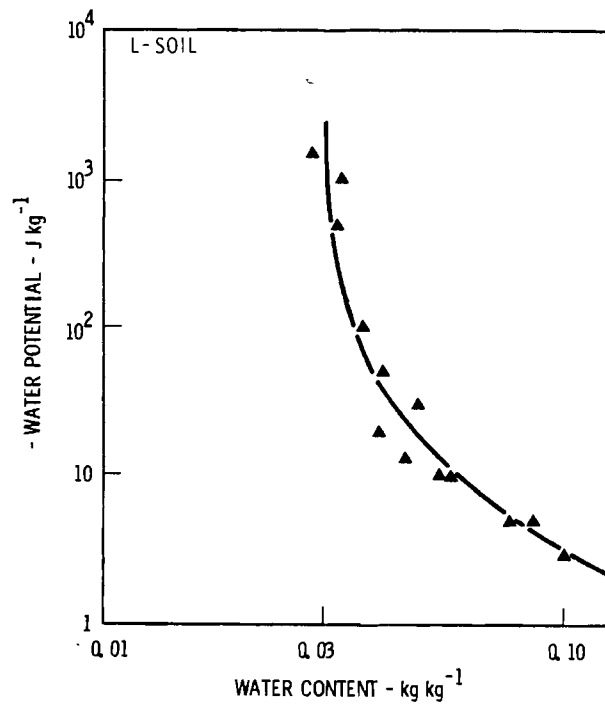


FIGURE 4.2. Soil Water Retention Curve for L-Soil Hanging Water Column and Pressure Plate Data

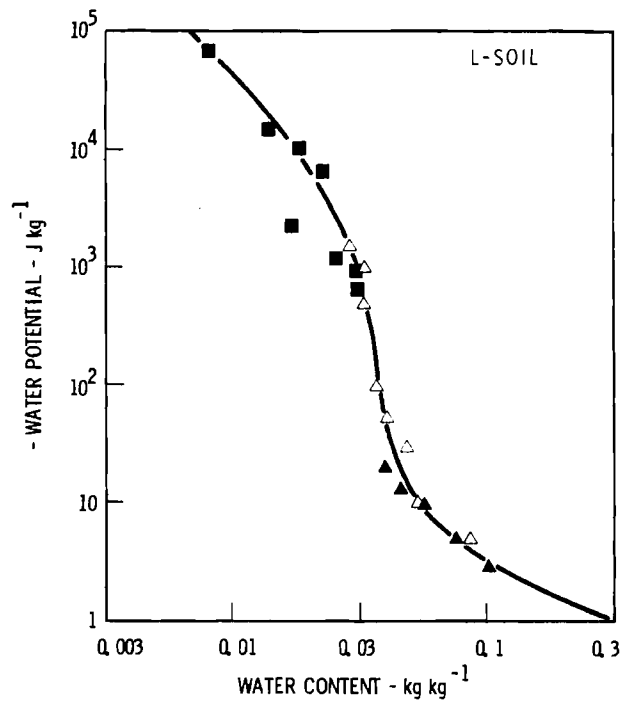


FIGURE 4.3. Soil Water Characteristic Curve for L-Soil (Curved fitted by Equation 4.1). \blacktriangle hanging water column, \triangle pressure plate, \blacksquare thermocouple psychrometer

This equation is strictly empirical with no physical significance to the parameters used, however it does provide a good fit for the entire potential range. Figure 4.4 shows a comparison of the soil water characteristic function of B-soil (Quincy) and L-soil (BWTF). The shape of the L-soil curve relative to the B-soil curve is very similar even though the L-soil has a lower bulk density. This is indicative of the coarser nature of the L-soil.

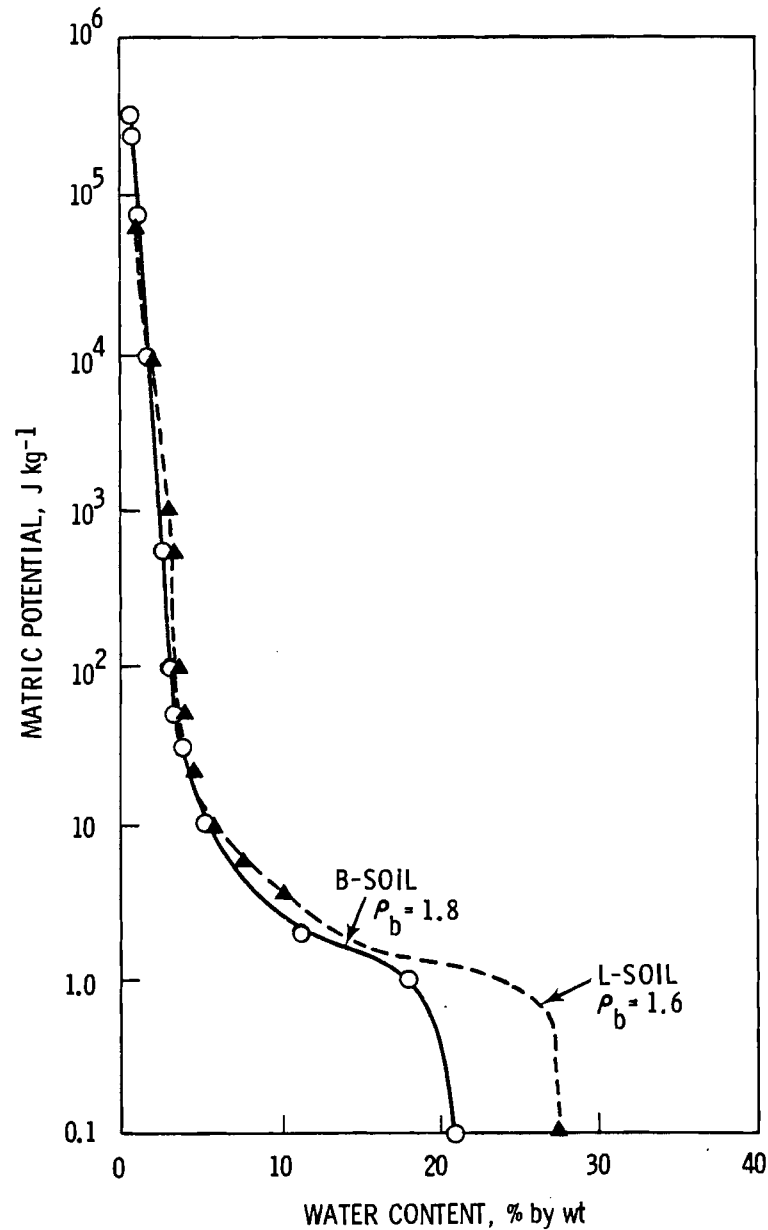


FIGURE 4.4. Comparison of the Soil Water Characteristic Function for B-Soil (Gee and Campbell 1980), and L-Soil

4.3 HYDRAULIC CONDUCTIVITY

The value of saturated hydraulic conductivity obtained by the falling head method was $1.4 \times 10^{-4} \text{ m s}^{-1} \pm 0.2 \times 10^{-4}$. This compares very well with $1.7 \times 10^{-4} \text{ m s}^{-1}$ reported for L-soil by Jones et al. (1979), for a similar method. The estimates of saturated conductivity obtained from the advance of the wetting front experiments were not so encouraging. The average value of m obtained for the vertical advance of the wetting front was $0.28 \text{ cm sec}^{-1/2}$. This produces an estimate of k_s of $1.56 \times 10^{-5} \text{ m s}^{-1}$ by equation 3.4, which is one order of magnitude below the other estimates. Jones et al. (1979) reported an m -value of 0.91 for the horizontal advance of a wetting front, (also suggested by Bresler et al. 1978). Using equation 3.4 gives a k_s of $1.85 \times 10^{-3} \text{ m s}^{-1}$, one order of magnitude above the other estimates. This large spread in estimates of k_s is distressing, however not uncommon. The advance of the wetting front method is not recommended using either horizontal or vertical infiltration. The more standard methods of Klute (1965) seem to produce more reproducible estimates.

The unsaturated conductivity function can be estimated from equation 3.3 or one very similar. Gee et al. 1981 found that the method of Campbell (1974), (i.e., $\beta = 2b + 3$) compared with direct measurement techniques better than Bresler (1978) (i.e., $\beta = 7.2$). This may be misleading; however, because the relative saturation term θ/θ_s was used. This is equivalent to setting the residual water content (θ_d) equal to zero. This increases the conductivity of the dry soil. This may account for the better fit shown by Gee et al. (1981), rather than a better choice of β . The choice of θ_d certainly biased the method of van Genuchten as shown by Gee et al. (1981). Until more direct conductivity measurements are made for L-soil at low water contents it will not be known how best to choose β .

4.4 THERMAL CONDUCTIVITY

Measured thermal conductivity values for the BWTF soil are shown in Table 4.3 and plotted in Figure 4.5 as a function of water content. There is generally good correspondence between this data (25°C) and thermal conductivity values published by Bouse (1975) for Hanford sediments (22°C, sand SX-S).

TABLE 4.3. Thermal Conductivity and Diffusivity of BWF Soil

Water Content		Bulk Density	Thermal Diffusivity	Thermal Conductivity
θ_m	θ_v			
kg kg^{-1}	$\text{m}^3 \text{m}^{-3}$	Mg m^{-3}	$\text{m}^2 \text{s}^{-1} \times 10^6$	$\text{W m}^{-1} \text{K}^{-1}$
0.0017	0.0027	1.59	0.194	0.159
0.0073	0.0116	1.59	0.191	0.163
0.0130	0.0207	1.59	0.200	0.179
0.0233	0.0264	1.56	0.263	0.233
0.0246	0.0379	1.54	0.297	0.272
0.0375	0.0611	1.63	0.360	0.397
0.0500	0.0795	1.59	0.430	0.490
0.0576	0.0922	1.60	0.447	0.537
0.0923	0.147	1.60	0.502	0.718
0.104	0.166	1.60	0.504	0.761
0.148	0.249	1.68	0.468	0.908
0.165	0.265	1.61	0.463	0.895
0.182	0.304	1.60	0.478	0.997
0.199	0.318	1.60	0.450	0.965
0.201	0.318	1.58	0.435	0.924
0.206	0.323	1.57	0.449	0.958

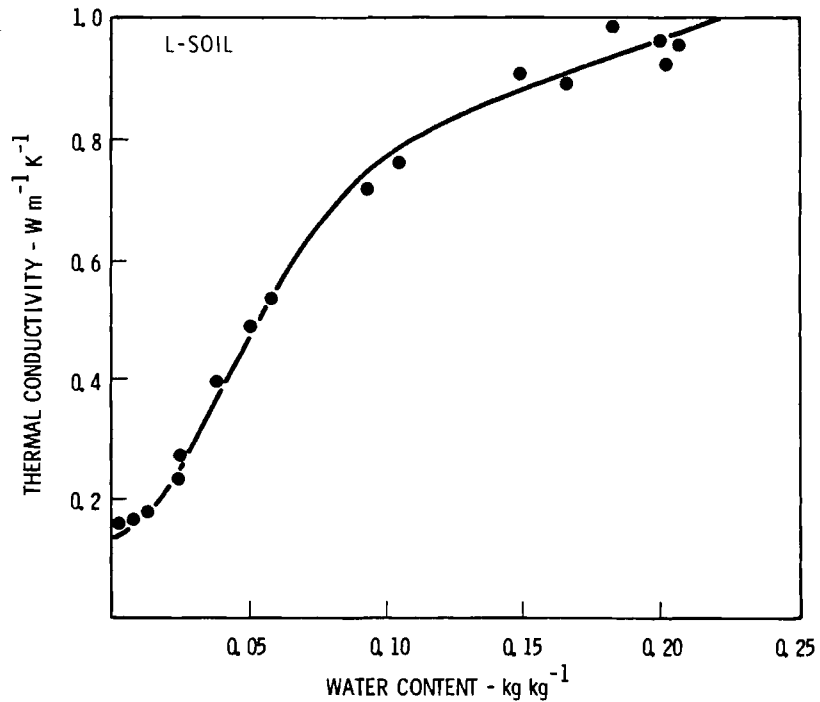


FIGURE 4.5. Thermal Conductivity of L-Soil as a Function of Water Content, Determined Over the Temperature Range 21 to 26°C

These thermal conductivity data conform to the numerical model obtained by McInnis (1981) and were fitted to the function

$$k_T = A + B\theta_m - (A-D) \exp [-(C\theta_m)^x] \quad (4.2)$$

where the parameter values of the curve of Figure 4.3 are $A = 0.64 \text{ W m}^{-1}\text{K}^{-1}$, $B = 1.63 \text{ W m}^{-1}\text{K}^{-1} (\text{kg kg}^{-1})$, $D = 0.135 \text{ W m}^{-1}\text{K}^{-1}$, $C = 17$ and $x = 2$.

This equation provides a method of describing the water content dependence of thermal conductivity analytically. Equation 4.2 can also be used with equations 3.5 and 3.6 to calculate the thermal diffusivity.

5.0 CONCLUSIONS

The soil material used to fill the BWTF lysimeters is a composite of the top 8 meters of soil and sediment excavated during construction. The original profile consisted of 1-2 meters of medium sands belonging to the Quincy soil series. The remainder of the profile was catastrophic flood deposits known as the Pasco Gravels. The resulting composite mix is a very coarse textured sand showing low water holding capacity, high saturated hydraulic conductivity, and low air-dry thermal conductivity.

The soil characteristic function shows that the soil can be drained to a saturation ratio of 0.4 at a water potential of only -3.0 J/kg. The S-shaped curve generated is difficult to describe analytically with standard equations; however, the midrange water contents can be expressed as a function of water potential using standard power functions. If the entire curve including low and high water contents are to be described, more complicated equations must be used. One approach is to allow the residual water content to vary with potential. Analytic expressions can be obtained which allow the calculation of the soil water diffusivity.

The hydraulic conductivity may be described by the power function approach with the saturated conductivity being measured by standard procedures. The conductivity data reported here is consistent with other data reported for similar soils found on the Hanford site.

Thermal conductivity measurements are consistent with predicted trends. The increasing values with increasing data content and the range of values are indicative of sandy soils. An analytic expression is given which provides an empirical, but accurate method of describing the thermal conductivity and for calculating the thermal diffusivity.

REFERENCES

- Blake, G. R. 1965. Particle Density. In: C. A. Black et al. (eds.). Methods of Soil Analysis. Agronomy No. 9, Part I, pp. 371-374. Am. Soc. Agron., Madison, Wisconsin.
- Bouse, D. G. 1975. Thermal Conductivity of Hanford Waste Tank Solids and Six Tank Farm Soil Samples. Report ARH-CD-378. Atlantic Richfield, Hanford Co., Richland, Washington.
- Bresler, E., D. Russo and R. D. Miller. 1978. Rapid Estimate of Unsaturated Hydraulic Conductivity Function. *Soil Sci. Soc. Am. Proc.* 42:170-172.
- Buckingham, E. 1907. Studies on the Movement of Soil Moisture. U.S. Department of Agriculture. Bureau of Soils - Bulletin No. 38.
- Campbell, G. S. 1974. A Simple Method for Determining Unsaturated Conductivity from Moisture Retention Data. *Soil Sci.* 117:311-314.
- Campbell, G. S., and A. M. Wilson. 1972. Water Potential Measurements of Soil Samples. In: Brown, R. W., and B. P. Van Haveren (eds.) Psychrometry in Water Relations Research, Utah State University, pp. 142-149.
- Day, P. R. 1965. Particle Fractionation and Particle-Size Analysis. In: C. A. Black et al. (eds.). Methods of Soil Analysis. Agronomy No. 9, Part I, pp. 545-576. Am. Soc. Agron. Madison, Wisconsin.
- De Vries, D. A. 1963. Thermal Properties of Soils, In W. R. Van Wyck (ed). *Physics of Plant Environment*. North Holland Publishing Co., Amsterdam. pp. 210-235.
- Gee, G. W., and J. W. Bauder. 1979. Particle Size Analysis by Hydrometer: A Simplified Method for Routine Textural Analysis and a Sensitivity Test of Measurement Parameters. *Soil Sci. Soc. Am. Proc.* 43:1006-1007.
- Gee, G. W., and A. C. Campbell. 1980. Monitoring and Physical Characterization of Unsaturated Zone Transport - Laboratory Analysis. PNL-3304. Pacific Northwest Laboratory, Richland, Washington 99352.
- Gee, G. W., A. C. Campbell, P. J. Wierenga and T. L. Jones. 1981. Unsaturated Moisture and Radionuclide Transport: Laboratory Analysis and Modeling. Report PNL-3616, UC-70, Battelle, Pacific Northwest Laboratory, Richland, Washington.
- Hajek, B. F. 1966. Soil Survey - Hanford Project in Benton County, Washington. BNWL-243, Pacific Northwest Laboratory, Richland, Washington 99352.

- Jones, T. L., W. A. Jordan and G. W. Gee. 1979. A Test of the Bressler-Russo-Miller Method for Unsaturated Conductivities. Report RHO-SA-125, Rockwell International, Richland, Washington.
- Jones, T. L., W. A. Jordan, A. H. Lu, and J. B. Sisson. 1981. Predictions of Infiltration and Drainage Using Field and Laboratory Measured Hydraulic Parameters. RHO-SA-164. Rockwell Hanford Operations, Richland, Washington 99352
- Klute, A. 1965. Laboratory Measurement of Hydraulic Conductivity of Saturated Soil, In: Black, C. A. et al. (eds). Methods of Soil Analysis, Agronomy No. 9, Part I, pp. 220-221. Am. Soc., Agron. Madison, Wisconsin.
- Kocher A. E., and A. J. Strahorn. 1919. Soil Survey of Benton County, Washington. U.S. Government Printing Office.
- McInnis, K. 1981. Thermal Conductivities of Soils from Dryland Wheat Regions in Eastern Washington. M.S. Dissertation, Washington State University, Pullman, Washington.
- Parikh, R. J., J. A. Havens and H. D. Scott. 1979. Thermal Diffusivity and Conductivity of Moist Porous Media. *Soil Sci. Soc. Am. J.* 43:1050-1052.
- Phillips, S. J., A. C. Campbell, M. D. Campbell, G. W. Gee, H. H. Hooper, and K. O. Schwarzmiller. 1979. A Field Test Facility for Monitoring Water/Radionuclide Transport Through Partially Saturated Geologic Media: Design, Construction and Preliminary Description. Report PNL-3226-UC70. Battelle, Pacific Northwest Laboratory, Richland, Washington.
- Phillips, S. J., L. L. Ames, R. E. Fitzner, G. W. Gee, G. A. Sandess, and C. S. Simmons. 1980. Characterization of the Hanford 300 Area Burial Grounds. Final Report Decontamination and Decommissioning. PNL-2557. Pacific Northwest Laboratory, Richland, Washington 99352
- Richards, L. A. 1931. Capillary Conduction of Liquids Through Porous Mediums. *Physics.* 1:318-333.
- Riha, S. J., K. J. McInnes, S. W. Childs and G. S. Campbell. 1980. A Finite Element Calculation for Determining Thermal Conductivity. *Soil Sci. Soc. Am. Proc.* 44:1323-1325.
- Tallman, A. M., K. R. Fecht, M. C. Marratt, and G. V. Lest. Geology of the Separation Areas, Hanford Site, South Central Washington, RHO-ST-23. Rockwell Hanford Operations, Richland, Washington 99352
- Vomocil, J. A. 1965. Porosity. In: Black, C. A. et al. (eds). Methods of Soil Analysis. Agronomy No. 9, Part I, pp. 299-307. Am. Soc. Agron. Madison, Wisconsin.

APPENDIX A

THE COUPLED FLOW OF HEAT AND WATER

APPENDIX A

THE COUPLED FLOW OF HEAT AND WATER

A.1. FLUX OF WATER

The mathematical-physical approach to description of mass and energy transport requires firstly, selection of relations between the components of mass flux and the driving forces and secondly, combination of these flux relationships with the mass balance equation (Klute 1973). The macroscopic differential balance of mass for transport in a rigid porous medium, where the material is present in n phases is (Raats 1975)

$$\frac{\partial \rho_i}{\partial t} = \nabla \cdot q_i + E_i \quad (\text{A.1})$$

$$i = 1, 2, \dots, n$$

The individual mass flux densities of i are

$$q_i = -D_i (\nabla \rho_i) \quad (\text{A.2})$$

and the total mass flux density is

$$q = -\sum D_i (\nabla \rho_i) \quad (\text{A.3})$$

Application of these equations to soil systems consistent with the modeling objectives of this investigation requires the following assumptions:

1. the soil matrix behaves as a rigid porous body
2. the medium is isotropic with respect to diffusion
3. the air phase is at constant pressure so that convective transport of water vapor is negligible

4. storage of water in the gas phase is negligible
5. concentration of solutes in the liquid phase is negligible
6. the solution phase is of constant macroscopic average density
7. mass density gradient of water can be expressed as a function of water concentration gradient, temperature gradient and body force fields (gravitational)
8. coefficients of diffusion are independent of their respective driving forces and the position of the driving forces (concentration and temperature gradients) but may depend on other variables such as concentration, temperature, air content, air pressure and gas-filled pore space geometry (Klute 1973).

Applying these assumptions to equation A.3 for a system of vapor and liquid water and expressing flux density on a volume basis gives

$$J_w = J_l + J_v = -(D_{\theta} \nabla \theta + K_{\theta} i_z) - (D_T \nabla T) \quad (\text{A.4})$$

The first term on the right hand side is the isothermal component and the second the thermal component of water flux. If the diffusion coefficients are partitioned according to liquid and vapor flux

$$J_w = -(D_{\theta l} \nabla \theta + D_{Tl} \nabla T + K_{\theta} i_z) - (D_{\theta v} \nabla \theta + D_{Tv} \nabla T) \quad (\text{A.5})$$

then independent expression for liquid (first term on right hand side of equation A.5) and vapor (second term) volume flux density are obtained (Philip and De Vries 1957).

A.2 ISOTHERMAL TRANSPORT OF WATER

The isothermal component of the Philip-De Vries (1957) model is

$$J_{ew} = -D_{\theta} \nabla \theta - K_{\theta} i_z \quad (\text{A.6})$$

and if flux density of both vapor and liquid are distinguished

$$J_{\theta w} = (J_{\theta l}) + (J_{\theta v}) = (-D_{\theta l} \nabla \theta - K_{\theta} i_z) + (-D_{\theta v} \nabla \theta) \quad (\text{A.7})$$

The expression for transport of liquid at constant temperature

$$J_{\theta l} = -D_{\theta l} \nabla \theta - K_{\theta} i_z \quad (\text{A.8})$$

arises directly from Darcy's law, which is usually expressed in potential form as

$$\begin{aligned} J_{\theta l} &= -K_{\theta} \nabla \psi \\ &= -K_{\theta} \nabla \psi_p - K_{\theta} \frac{d\psi_g}{dz} \\ &= -K_{\theta} \frac{d\psi_p}{d\theta} \nabla \theta - K_{\theta} i_z \end{aligned} \quad (\text{A.9})$$

The isothermal diffusion coefficient is therefore the familiar soil water diffusivity

$$D_{\theta l} = K_{\theta} \frac{d\psi_p}{d\theta} \quad (\text{A.10})$$

The slope of the soil water retention curve ($d\psi_p/d\theta$) is hysteretic and $D_{\theta l}$ is dependent on the wetting or drying history of the system (Jury 1973). No theoretical basis exists for calculation of $D_{\theta l}$. It is usually determined directly by measurement of steady state liquid flow rate and water content gradients or it may be calculated from measured hydraulic conductivity and the soil water retention curve (equation A.10).

Isothermal vapor diffusivity is smaller than liquid diffusivity at high water contents but becomes dominant at lower water contents (De Vries 1958;

Jackson 1964a, b). For this reason, neglect of isothermal vapor flux at intermediate and low water contents will not be appropriate in modeling water movement at the BWTF site.

The expression of isothermal vapor flux is

$$J_{\theta v} = -D_{\theta v} \nabla \theta \quad (\text{A.11})$$

Philip and De Vries (1957) expanded this expression by using

$$\nabla \rho_v = h \nabla \rho_v^0 + \rho_v^0 \nabla h \quad (\text{A.12})$$

$$\rho = \rho_v^0 h = \rho_v^0 \exp\left(\frac{\psi M g}{R T}\right) \quad (\text{A.13})$$

and if h is a function of θ only and ρ_v^0 a function of T only (Philip 1955)

$$\begin{aligned} J_{\theta v} &= -\left[D_{va} \gamma \left(\frac{M g}{R T} \right) \left(\frac{\rho_v^0}{\rho_l} \right) \left(\frac{dh}{d\theta} \right) (a + \theta f) \right] \nabla \theta \\ &= -\left[D_{va} \gamma \left(\frac{M^2 g^2}{R^2 T^2} \right) \left(\frac{\rho_v^0}{\rho_l} \right) \left(\frac{d\psi}{d\theta} \right) (a + \theta f) \right] \nabla \theta \end{aligned} \quad (\text{A.14})$$

The value of $D_{\theta v}$ over the range of water content for which $0.99 < h < 1.0$ is very small and is usually neglected in evaluating water flux. However when $h < 0.99$, $dh/d\theta$ rises to a maximum value, then decreases to zero as θ and h approach zero. For this reason, D_{θ} usually exhibits a secondary maximum in the dry range of water content. Because of this effect, $D_{\theta v}$ contributes equally with $D_{\theta l}$ to flux at low water contents, and has accordingly enjoyed considerable research attention.

A.3 THERMAL TRANSPORT OF WATER

The expression for thermal transport of mass at constant water content is

$$J_{Tw} = -D_T \nabla T \quad (A.15)$$

and for a homogenous, isotropic medium consisting of liquid and vapor only

$$\begin{aligned} J_{Tw} &= (-D_{Tl} \nabla T) + (-D_{Tv} \nabla T) \\ &= J_{Tl} + J_{Tv} \end{aligned} \quad (A.16)$$

The volume flux of liquid under the influence of a temperature gradient may be quite considerable in relation to that of vapor (see Philip and De Vries 1957) but maximum values of D_{Tl} are observed at high water contents where $D_{\theta l}$ is very much larger, while at low water contents D_{Tv} is considerably larger. For these reasons, D_{Tl} may be ignored in modeling water flux, provided large and persistent unidirectional temperature gradients are not present.

The major contribution to water flux under nonisothermal conditions is from thermal vapor diffusion, D_{Tv} , which is influenced by two enhancement mechanisms: temperature enhancement and porosity enhancement or "series-parallel" flow.

Microscopic temperature gradients within air-filled pores are higher than the macroscopic gradient across the medium because the thermal conductivities of liquid and solid components of the system are higher than the thermal conductivity of the vapor-filled pore space ($\lambda_l = 5.92 \times 10^{-1}$; $\lambda_s = 2.94$ to 8.40 ; $\lambda_a = 1.74 \times 10^{-2} \text{ J m}^{-1} \text{ s}^{-1} \text{ }^\circ\text{C}^{-1}$). This results in vapor flux that is as much as twice that predicted by Ficks law. The temperature gradient enhancement factor is defined as (De Vries 1952).

$$\zeta = \frac{(\nabla T)_a}{a(\nabla T)_a + \theta(\nabla T)_\theta + s(\nabla T)_s} \quad (A.17)$$

It should be appreciated, from the form of equation A.13 that the maximum value of ζ approaches $1/\phi$ at $\theta = 0$ (De Vries and Philip 1959). Because of the larger thermal conductivity of quartz, the temperature gradient enhancement of vapor flow is some 3 to 34% higher for quartz-rich soils. Maximum values occur in dry, compact soils.

Philip and De Vries (1957) introduced the concept of "series-parallel" flow of water through vapor-filled pores and discontinuous liquid islands. Internal condensation and evaporation allows a diffusion volume that is the sum of air and liquid pore space up to a liquid content at which islands become continuous (θ_k or a_k). This enhancement effect is expressed as a porosity term ($a + \theta f$) that replaces a in the De Vries (1950) model, where

$$f = 1 \text{ for } a > a_k \text{ or } \theta < \theta_k$$

$$f = \frac{a}{a_k} \text{ for } a < a_k \text{ or } \theta > \theta_k$$

θ_k was interpreted by Philip and De Vries (1957) as that θ value at which K_θ falls to some "small, but arbitrary fraction of its saturation value." Jury and Letey (1979) modified the porosity enhancement expression to include an adjusted path length of diffusion (ξ) depending on whether flux is through a vapor- or liquid-filled space. The currently accepted expression for the enhancement factor is therefore

$$\beta = v \zeta \xi (a + \theta f) \tag{A.18}$$

where

$$\xi = \left[\frac{a + \theta f}{a + \theta f \left(\frac{\lambda}{\lambda_1} \right)} \right]^2 \tag{A.19}$$

Combining the expression for Fick's law of diffusion with the Philip-De Vries model and the modifications of Jury and Letey (1979) gives

$$D_{Tv} = D_{va} \beta \left(\frac{Mg}{RT} \right) h \frac{d\rho_v^0}{dT} = D_{va} \beta h \rho_v^0 \left(\frac{Mg}{R^2 T^3} \right) \quad (A.20)$$

There exists no means for direct measurement of D_{Tv} , but several attempts have been made to measure β and use the values to calculate D_{Tv} . Unfortunately, values obtained for β have been contradictory (Jury and Letey 1979; Cary 1979), and the size of this factor for intermediate water content remains uncertain. An idealized summary of the various conditions that may exist in soil is provided in Table A.1 together with qualitative estimates of water content, diffusion coefficients and the enhancement factor.

A.4 HEAT CONDUCTION

The transport of heat in a continuous medium is described by Fourier's law

$$J_h = -\lambda \nabla T = D_{hT} \rho c \nabla T \quad (A.21)$$

In noncontinuous, multiple-component media such as soil containing both liquid and gas phase water and air, transport of heat may be enhanced by flux of the mobile components (convective flux of heat). However, if contact between the solid components is limited, conductive transport may be retarded. For this reason thermal conductivity of soil is dependent on the relative proportions of solid, liquid and gas and the nature and arrangement (mineralogy, packing and particle size distribution) of solid particles (Baver et al. 1972). Measured heat flux in soil is therefore the combined effect of several processes occurring at specific locations within the soil body. It is necessary therefore to consider the interaction of heat and water flux in modeling water movement.

A.5 COUPLED HEAT AND WATER FLUX

The macroscopic differential balance of heat is (Raats 1975)

TABLE A.1. Diagrammatic Representation and Qualitative Description of Vapor and Liquid Flow Quantities (modified after Rose 1963)

DIAGRAMATIC	STAGE	TYPE OF FLOW	a_1	h	D_{a1}^*	D_{T1}^*	D_{aV}^*	D_{TV}^*	β^{**}
	ADSORPTION OF WATER ON PORE WALLS AND FREE WATER VAPOR PRESENT IN THE PORE	VAPOR FLOW OBEYING FICK'S LAW	$0 < a < a_k$	$0.2 < h < 0.6$	ZERO	ZERO	LOW	MEDIUM	$\alpha < \beta \leq 1$
	ISOLATED LIQUID ISLANDS	ENHANCED VAPOR FLOW	$0 < a < a_k$	$0.6 < h < 0.99$	ZERO	ZERO	HIGH	HIGH	$1 < \beta < 2$
	CONTINUOUS LIQUID FILMS	ENHANCED VAPOR AND UNSATURATED LIQUID FLOW	$a \approx a_k$	$0.6 \ll h < 0.99$	LOW	VERY LOW	LOW	HIGH	$\beta = 2$
	ISOLATED GAS AND VAPOR ISLANDS	UNSATURATED LIQUID FLOW AND SOME VAPOR FLOW	$a_k < a < a_s$	$0.99 < h < 1.0$	MEDIUM	MAXIMUM	VERY LOW	LOW	$0 < \beta < 2$
	SATURATED WITH LIQUID	SATURATED LIQUID FLOW AND NO VAPOR FLOW	$a = a_s$	---	MAXIMUM	ZERO (?)	ZERO	ZERO	ZERO

* MAGNITUDE OF DIFFUSION COEFFICIENTS ARE EXPRESSED RELATIVE TO THE MAXIMUM VALUE OF EACH INDIVIDUAL COEFFICIENT.

**ANTICIPATES VALUE

$$\frac{\partial H}{\partial t} = \nabla J_h \quad (\text{A.22})$$

where H as a function of temperature is

$$H = \sum L_{i\alpha} (T) \rho_i + c_i (T - T_0) \quad (\text{A.23})$$

The heat flux density J_h is the sum of a diffusive component and a convective component given by

$$J_h = J_{hd} + J_{hc} \quad (\text{A.24})$$

Using Fourier's law for the diffusive component ($J_{hd} = -\lambda \nabla T$) and expressions for the flux of heat in convection of matter $[(T - T_0) c_{\alpha i} \sum J_i]$ and during phase transitions $[\sum L_{i\alpha} (T) J_i]$, equation A.24 becomes

$$J_h = -\lambda \nabla T + (T - T_0) c_{\alpha i} \sum J_i + \sum L_{i\alpha} (T) J_i \quad (\text{A.25})$$

In a system of soil, liquid water, and water vapor De Vries (1958) expressed equation A.25 as

$$J_h = -(\lambda_* + L_T \rho_l D_{TV}) \nabla T + c_l \nabla T J_l \rho_l + L_T J_v \rho_l \quad (\text{A.26})$$

where, in terms of the flux enhancement theory of Jury and Letey (1979)

$$\lambda_{JV} = L_T \rho_l D_{TV} = L_T \rho_l h \left(\frac{Mg}{RT} \right) \left(\frac{d\rho_v^0}{dT} \right) D_{va}^\beta \quad (\text{A.27})$$

where λ_{JV} is the contribution to heat flux by vapor distillation and where only transfer of sensible heat by liquid flux (second term in equation A.26) and transfer of latent heat by vapor flux (third term) are considered significant components of heat flux.

Clearly the flux of heat and water interact inseparably in soil and a complete theory requires simultaneous description of both components. De Vries (1958) provided the heat flux component of the Philip-De Vries model and linked this to flux of water. In order to distinguish between flux of vapor and liquid, the following continuity equations apply to a homogenous system of liquid and vapor in the absence of salt gradients:

$$\frac{\partial \theta_l}{\partial t} = - \nabla J_l - E_v \quad (\text{A.28})$$

$$\frac{\partial \theta_v}{\partial t} = - \nabla J_v + E_v \quad (\text{A.29})$$

$$\frac{\partial \theta}{\partial t} = - \nabla J_w \quad (\text{A.30})$$

and if liquid and vapor are always in equilibrium

$$\theta_v = (\phi - \theta_l) \frac{\rho_v^0 h}{\rho_l} \quad (\text{A.31})$$

Using equations A.28, A.29, A.30 and A.31, De Vries (1958) formulated the equations that govern simultaneous transfer of water and heat in porous media as: Flux of water:

$$\left[1 + \frac{D_{\theta v}}{\alpha \gamma D_{va}} - \frac{\rho_v}{\rho_l} \right] \frac{\partial \theta_l}{\partial t} + \left[\frac{(\phi - \theta_l) h \left(\frac{d\rho_v^0}{dT} \right)}{\rho_l} \right] \frac{\partial T}{\partial t} \\ = \nabla (D_{\theta} \nabla \theta_l) + \nabla (D_T \nabla T) + \frac{\partial K_{\theta}}{\partial z} \quad (\text{A.32})$$

Flux of heat:

$$\begin{aligned}
 & \left[C + L_T (\phi - \theta_1) h \frac{d\rho_v^0}{dT} \right] \frac{\partial T}{\partial t} + \left[\frac{L\rho_1 D_{\theta v}}{\alpha \gamma D_{va}} - L_T \rho_v + \rho_1 g \left(\psi_p - T \frac{\partial \psi_p}{\partial T} \right) \right] \frac{\partial \theta}{\partial t} \\
 & = \nabla \left[(\lambda_* + \lambda_{Jv}) \nabla T \right] + L_T \rho_1 \nabla (D_{\theta v} \nabla \theta_1) \\
 & \quad + \rho_1 c_1 \left[(D_{\theta 1} \theta_1 + D_{T1} \nabla T + K_{\theta} i_z) \nabla T \right] \tag{A.33}
 \end{aligned}$$

These equations can only be regarded as approximate because they quantify several mechanisms which are not additive (Jury 1973) and in addition, the coefficients needed in these equations are extremely difficult and expensive to obtain.

In a simulated, steady-state heat conduction experiment with Yolo light clay and a medium sand, De Vries (1958) showed that the interaction between heat and water transfer depended on the following factors:

1. boundary conditions for water transfer
2. direction of the temperature gradient
3. ratio of the two coefficients of diffusivity D_{θ} and D_T .

For horizontal water and heat flux, the water content gradient was found to be small for a boundary condition $J_w = 0$, except where D_T is not small with respect to D_{θ} . In the case of Yolo light clay, this region lies in the water content range $0.1 < \theta < 0.2$, and for the sand in the range $0 < \theta < 0.1$. In the region where $D_{\theta 1} \ll D_{\theta v}$, flux of water is mainly in the liquid form and vapor diffusion due to a temperature gradient will contribute to heat transfer. Equation A.26 is appropriate to describe heat flux density, and since $L\rho_1 D_{\theta v} D_T / D_{\theta} \ll \lambda$, the apparent conductivity (λ) measured under these conditions is the same as that predicted from $(\lambda_* + \lambda_{Jh})$. The water content and temperature gradients in the x-direction are given by

$$\frac{d\theta_1}{dx} = \frac{J_h D_T}{\lambda D_{\theta} - L\rho_1 D_{\theta v} D_T} \tag{A.34}$$

$$\frac{dT}{dx} = \frac{J_h D_\theta}{\lambda D_\theta - L \rho_l D_{\theta v} D_T} \quad (\text{A.35})$$

For horizontal flow in the region where $D_{\theta l} \ll D_{\theta v}$, water flows mainly as vapor, and in this region $D_{Tl} \ll D_{Tv}$, usually. There is therefore no net vapor movement and the appropriate equation for heat flux density is

$$J_h = -\lambda_* \nabla T + L_{T_0} J_v + C_l (T - T_0) J_w \quad (\text{A.36})$$

where λ_* represents thermal conductivity of the porous medium when no water flux occurs. The water content and temperature gradients are now

$$\frac{d\theta_l}{dx} = J_h \frac{D_{Tv}}{\lambda_*} D_{\theta v} \quad (\text{A.37})$$

$$\frac{dT}{dx} = \frac{-J_h}{\lambda_*} \quad (\text{A.38})$$

In the region where $D_{\theta l}$ is of approximate equal magnitude to $D_{\theta v}$, $D_{Tl} \ll D_{Tv}$ and return flow in response to the temperature-induced vapor flow will take place both as vapor and liquid. Here vapor diffusion will contribute only partly to the transfer of heat and for steady state flow and $J_w = 0$,

$$\lambda = \lambda_a + \lambda_{Jh} = \lambda_a + \frac{D_{\theta l} h \rho_l \left(\frac{d\rho_v^0}{dT} \right) L_T D_{va} \left(\frac{Mg}{RT} \right) \beta}{D_\theta} \quad (\text{A.39})$$

A similar analysis for vertical flux of heat and water, in relation to the same regions discussed for the horizontal case gives:

1. region $D_{\theta l} \ll D_{\theta v}$: K is very small and transfer of heat and water will be equal to that in the horizontal case, provided flux is steady

2. region $D_{\theta 1} \gg D_{\theta v}$ or of comparable magnitude, will not exhibit proportionality between J_h and ∇T and results will depend on boundary conditions and gradient directions.

For vertical, transient state flux where $D_{\theta 1} \gg D_{\theta v}$, equations A.26 and A.32 will apply but where $D_{\theta 1} \ll D_{\theta v}$ or $D_{\theta 1} \sim D_{\theta v}$, the result will depend on the experimental conditions.

SYMBOL NOTATION

a	Volumetric air content of the medium (m^3 air m^{-3} bulk soil)
a_k	Volumetric air content at which vapor spaces become continuous ($m^3 m^{-3}$)
c	Volumetric heat capacity associated with the reference system α , given by $c = c_s \rho_s + c_{\alpha} \rho_{\alpha}$ ($J m^{-3} ^\circ C^{-1}$)
c_{α}	Volumetric heat capacity of water in the reference state α ($J m^{-3} ^\circ C^{-1}$)
c_l	Specific heat of liquid water ($J kg^{-1} ^\circ C^{-1}$)
c_s	Specific heat of bulk soil (taken as $0.9 \times 10^3 J kg^{-1} ^\circ C^{-1}$)
c_v	Specific heat of water vapor at constant pressure (taken as $4.18 \times 10^3 J kg^{-1} ^\circ C^{-1}$)
D_i	Diffusion coefficient for component i
D_T	Thermal diffusivity of water ($m^2 s^{-1}$)
D_e	Isothermal diffusivity of water ($m^2 s^{-1}$)
D_{el}	Isothermal liquid diffusivity ($m^2 s^{-1}$)
D_{ev}	Isothermal vapor diffusivity ($m^2 s^{-1}$)
D_{Tv}	Thermal vapor diffusivity ($m^2 s^{-1}$)
D_{Tl}	Thermal liquid diffusivity ($m^2 s^{-1}$)
D_{hT}	Heat diffusivity in response to a temperature gradient ($J m^{-2} s^{-1}$)
D_{va}	Molecular diffusivity of water vapor in air ($m^2 s^{-1}$)
E_i	Supply of material to phase i from other phases
E_v	Evaporation rate (s^{-1})
f	A dimensionless factor which adjusts the liquid space contribution to vapor flow
g	Acceleration of gravity ($m s^{-2}$)

H	Heat content per unit volume (J m^{-3})
h	Relative humidity $h = \exp(\psi g/RT)$
i_z	Unit vector in the z direction
J_h	Flux density of heat ($\text{J m}^{-2} \text{s}^{-1}$)
J_i	Flux density of component i
J_{hd}	Diffusive heat flux density
J_{hc}	Convective heat flux density
J_l	Volume flux density of liquid water (m s^{-1})
J_v	Volume flux density of water vapor (m s^{-1})
J_{Tv}	Thermal volume flux density of vapor (m s^{-1})
J_{Tw}	Thermal volume flux density of water (m s^{-1})
$J_{\theta l}$	Isothermal volume flux density of liquid water (m s^{-1})
$J_{\theta w}$	Isothermal volume flux density of water (m s^{-1})
J_w	Volume flux density of water (liquid and vapor) (m s^{-1})
K_s	Saturated hydraulic conductivity
K_θ	Hydraulic conductivity as a function of water content (m s^{-1})
$L_{i\alpha}$	Latent heat released in the transfer of water at temperature T from phase i to reference state α (J kg^{-1})
L_0	Heat of vaporization at reference temperature T_0 (J kg^{-1})
L_T	Latent heat of vaporization of water (J kg^{-1}) $L_T = L_0 - (c_l - c_v)(T - T_0)$
M	Molecular mass of water ($0.018 \text{ kg mol}^{-1}$)
m_i	Slope of the capillary rise - time curve
q_i	Vector mass flux density of component i ($\text{kg m}^{-2} \text{s}^{-1}$)
R	Universal gas constant ($8.314 \text{ J mol}^{-1} \text{ K}^{-1}$)

s	Volumetric solid content of medium (m^{-3} solid m^{-3} bulk soil)
T	Absolute temperature (K)
t	Time (s)

GREEK SYMBOLS

α	Tortuosity factor
β	General enhancement factor
∇	Vector differential operator
ζ	Ratio of average temperature gradient of pore spaces to medium
θ	Water content of the medium
θ_k	Water content at which liquid films become continuous and vapor spaces discontinuous
θ_l	Volumetric liquid water content ($m^3 m^{-3}$)
θ_m	Specific water content of the medium (kg water kg^{-1} soil)
θ_s	Saturated water content
θ_v	Volumetric water content (m^3 water m^{-3} bulk soil)
λ	Thermal conductivity of soil including thermal distillation ($J s^{-1} m^{-1} ^\circ C^{-1}$)
λ_{jv}	Thermal conductivity due to vapor movement ($J m^{-1} s^{-1} ^\circ C^{-1}$)
λ_l	Thermal conductivity of liquid water ($J s^{-1} m^{-1} ^\circ C^{-1}$)
λ_a	Thermal conductivity of dry air ($J s^{-1} m^{-1} ^\circ C^{-1}$)
λ_s	Thermal conductivity of soil ($J s^{-1} m^{-1} ^\circ C^{-1}$)
λ_v	Thermal conductivity of saturated water vapor ($J s^{-1} m^{-1} ^\circ C^{-1}$)
λ^*	Hypothetical thermal conductivity of porous medium assuming no water movement
γ	Mass flow factor to allow for differences in boundary conditions governing air and vapor components of the diffusion system

ξ	Modified tortuosity factor introduced by Jury and Letey (1979)
ρ_b	Mass dry bulk density of soil (kg m^{-3})
ρ_i	The mass of water in phase i per unit bulk volume of porous medium (kg m^{-3})
ρ_l	Mass density of liquid water (kg m^{-3})
ρ_v	Mass density of water vapor (kg m^{-3})
ρ_θ	Mass density of saturated water vapor (kg m^{-3})
ϕ	Total porosity of porous medium (m^3 pore space m^{-3} bulk soil)
ψ	Total potential (J kg^{-1})
ψ_e	Air entry potential (J kg^{-1})
ψ_g	Gravitation potential (J kg^{-1})
ψ_p	Hydrostatic pressure potential of water (J kg^{-1})

REFERENCES FOR APPENDIX A

- Baver, L. D., W. H. Gardner, W. R. Gardner. 1972. Soil Physics. John Wiley and Son, New York. pp. 266-273.
- Cary, J. W. 1979. Soil Heat Transducers and Water Vapor Flow. *Soil Sci. Soc. Amer. J.* 43:835-839.
- De Vries, D. A. 1950. Some Remarks on Heat Transfer by Vapor Movement in Soils *Trans. 4th Int. Congr. Soil Sci.* 2:38-41.
- De Vries, D. A. 1952. Het Warmsegeleidingsvermogen van Grond. *Med. Landbouwhogeschool, Wageningen* 52:1-73.
- De Vries, D. A. 1958. Simultaneous Transfer of Heat and Moisture in Porous Media. *Trans. Amer. Geophys. Union.* 39:909-916.
- De Vries, D. A., and J. R. Philip. 1959. Temperature Distribution and Moisture Transfer in Porous Materials. *J. Geophys. Res.* 64:386-388.
- Jackson, R. D. 1964a. Water Vapor Diffusion in Relatively Dry Soil. I. Theoretical Considerations and Sorption Experiments. *Soil Sci. Soc. Am. Proc.* 28:172-176.
- Jackson, R. D. 1964b. Water Vapor Diffusion in Relatively Dry Soil. II. Description of experiments. *Soil Sci. Soc. Am. Proc.* 28:464-466.
- Jury, W. A. 1973. Simultaneous Transport of Heat and Moisture Through a Medium Sand. Ph.D. Dissertation, University of Wisconsin.
- Jury, W. A., and J. Letey, Jr. 1979. Water Vapor Movement in Soil: Reconciliation of theory and experiment. *Soil Sci. Soc. Amer. J.* 43:823-827.
- Klute, A. 1973. Soil Water Flow Theory and Its Application in Field Situations pp. 9-35. In: Bruce, R. R. et al (ed). *Field Soil Water Regime*. Special publication No. 5: *Soil Sci. Soc. Am.*
- Philip, J. R., and D. A. De Vries. 1957. Moisture Movement in Porous Materials Under Temperature Gradients. *Eos Trans. AGU*, 38:222-232.
- Raats, P. A. C. 1975. Transformations of Fluxes and Forces Describing the Simultaneous Transport of Water and Heat in Unsaturated Porous Media. *Water Res. Research.* 11:938-962.
- Rose, D. A. 1963. Water Movement in Porous Materials, II. The Separation of the Components of Water Movement. *Brit. J. Appl. Phys.* 14:491-496.

DISTRIBUTION

No. of
Copies

No. of
Copies

OFFSITE

A. A. Churm
DOE Chicago Patent Group
9800 South Cass Avenue
Argonne, IL 60439

C. R. Cooley
DOE Office of Nuclear
Waste Management
Washington, DC 10545

A. L. Dressin
DOE Office of Nuclear
Waste Management
Washington, DC 20545

C. H. George
DOE Office of Nuclear
Waste Management
Washington, DC 20545

C. A. Heath
DOE Division of Nuclear
Waste Management
Washington, DC 20545

S. Meyers
DOE Office of Nuclear
Waste Management
Washington, DC 20545

G. K. Ortel
DOE Office of Nuclear
Waste Management
Washington, DC 20545

D. R. Spurgeon
DOE Office of Nuclear
Waste Management
Washington, DC 20545

G. H. Daily
DOE Division of Waste Products
Washington, DC 20545

J. E. Dieckhoner
DOE Division of Waste Products
Washington, DC 20545

A. F. Kluk
DOE Division of Environmental
Control Technology
Washington, DC 20545

W. E. Mott
DOE Division of Environmental
Control Technology
Washington, DC 20545

R. W. Ramsey
DOE Division of Environmental
Control Technology
Washington, DC 20545

Department of Energy
Albuquerque Operations
Office
Albuquerque, NM 87115

Department of Energy
Chicago Operations Office
Argonne, IL 60439

Department of Energy
Idaho Operations Office
550 2nd Street
Idaho Falls, ID 83401

Department of Energy
Nevada Operations Office
Las Vegas, NE 89114

Department of Energy
Oak Ridge Operations Office
Oak Ridge, TN 37830

Department of Energy
Savannah River Operations
Office
Aiken, SC 29081

No. of
Copies

No. of
Copies

27 DOE Technical Information
Center

Technical Library
Argonne National Laboratory
Argonne, IL 60439

Atomic Industrial Forum, Inc.
7101 Wisconsin Avenue
Washington, DC 20014

Beverly Rawles
Battelle Memorial Institute
Office of Nuclear Waste
Isolation
505 King Avenue
Columbus, OH 43201

P. Columbo
Brookhaven National Laboratory
Upton, NY 11973

E. M. Romney
University of California
At Los Angeles
Westwood, CA 96137

Environmental Protection
Agency
Technology Assessment Division
Office of Radiation Programs
Washington, DC 20460

G. Levin
Idaho National Engineering
Laboratory
Idaho Falls, ID 83401

W. A. Jury
Department of Soils
University of California
Riverside
Riverside, California

J. B. Whitsett
Department of Energy
Idaho Operations Office
Idaho Falls, ID 83401

Technical Library
Idaho National Engineering
Laboratory
Idaho Falls, ID 83401

L. J. Johnson
Los Alamos National
Laboratory
Los Alamos, NM 87545

J. G. Steger
Los Alamos National
Laboratory
Los Alamos, NM 87545

Technical Library
Los Alamos National
Laboratory
Los Alamos, NM 87545

National Academy of Sciences
National Research Council
2101 Constitution Avenue
Washington, DC 20418

P. J. Wierenga
New Mexico State University
Las Cruces, NM 88003

5 G. S. Campbell
Washington State University
Pullman, WA 99164

5 A. Cass
Washington State University
Pullman, WA 99164

Nuclear Regulatory Commission
Division of Safeguards, Fuel
Cycle and Environmental
Research
Washington, DC 20545

J. W. Cary
USDA
Snake River Conservation
Research Center
Route 1, Box 186
Kimberly, Idaho 83341

No. of
Copies

C. Bishop
NRC Division of Fuel Cycle
Low Level Branch
Washington, DC 20555

F. J. Arsenault
Division of Safeguards, Fuel
Cycle and Environmental
Research
Washington, DC 20555

J. J. Davis
Division of Safeguards, Fuel
Cycle and Environmental
Research
Washington, DC 20555

F. Swenberg
Division of Safeguards, Fuel
Cycle and Environmental
Research
Washington, DC 20555

R. C. DeYoung
Division of Site Safety and
Environmental Analysis
Nuclear Regulatory Commission
Washington, DC 20555

R. P. Denlee
Division of Site Safety and
Environmental Analysis
Nuclear Regulatory Commission
Washington, DC 20555

D. E. Large
Oak Ridge National Laboratory
Oak Ridge, TN 37830

R. S. Lowrie
Oak Ridge National Laboratory
Oak Ridge, TN 37830

T. Tamura
Oak Ridge National Laboratory
Oak Ridge, TN 37830

No. of
Copies

Technical Library
Oak Ridge National Laboratory
Oak Ridge, TN 37830

E. L. Albenesius
Savannah River National
Laboratory
Aiken, SC 29081

Technical Library
Savannah River National
Laboratory
Aiken, SC 29081

ONSITE

2 Richland Operations Office
H. E. Ransom
E. A. Bracken

6 Rockwell Hanford Operations
J. L. Deichman
A. W. Graves
W. H. Price
D. D. Wodrich
S. J. Phillips
J. B. Sisson

2 United Nuclear Corporation
T. E. Dabroski
J. F. Nemec

46 Pacific Northwest Laboratory
T. D. Chikalla
G. W. Gee
T. L. Jones (10)
M. R. Kreiter
J. M. Latcovich
C. A. Novich
R. R. Kirkham
C. S. Simmons

No. of
Copies

A. M. Platt
W. R. Wiley
Technical Information (5)
Publishing Coordination (BE)(2)
Water and Land Resources
Library (20)